치의과학박사 학위논문

Effect of laminin-211–derived peptide on wound re-epithelialization in the early stages of cutaneous wound healing

라미닌-211 유래 펩티드가 피부창상 치유의 초기단계에서 재상피화에 미치는 영향

2020년 8월

서울대학교대학원

치의과학과 종양및발달생물학 전공

조 승 빈

ABSTRACT

Effect of laminin-211–derived peptide on wound re-epithelialization in the early stages of cutaneous wound healing

Seung Bin Jo

Department of Cancer and Developmental Biology

Graduate School

Seoul National University

(Directed by Prof. Byung-Moo Min, D.D.S., M.S., Ph.D.)

Peptides have been recognized as a valuable tool in the field of tissue engineering towards regenerating defective tissue. A minimal core bioactive peptide, PPFEGCIWN motif (Ln2-LG3-P2-DN3, residues 2678−2686) from the human laminin α2 chain, has been previously reported to promote cell attachment of normal human epidermal keratinocytes (NHEKs) and dermal fibroblasts (NHDFs), the major cell types that induce skin wound healing; however, the *in vivo* wound healing effects of the peptide has not yet been studied. In this

study, it has assessed whether a laminin-211-derived minimal core peptide could promote full-thickness cutaneous wound healing by accelerating wound closure and re-epithelization *in vivo*. In the cytocompatibility assessment, Ln2-LG3-P2-DN3-coated onto microfiber matrices showed significantly higher cell attachment and spreading activities compared with those of the vehicle or scrambled peptide-treated matrix in NHEKs and NHDFs. In the wound healing assessment, the wound areas of the Ln2-LG3-P2-DN3-treated rats were significantly smaller than that of the vehicle or scrambled peptide-treated rats on days 2 and 3 after wounding. Further, re-epithelization occurred significantly faster in Ln2-LG3-P2-DN3-treated rats than that of the vehicle or scrambled peptide-treated rats on day 3, and it was proportional to phospho-FAK-Tyr397 and active Rac1 expression. Moreover, in the Ln2-LG3-P2-DN3-treated rats, there were only minute amounts of inflammatory cell infiltration, compared to the controls. These findings support that the PPFEGCIWN motif is very effective in accelerating skin wound healing by enhancing wound closure and re-epithelization.

Keyword: PPFEGCIWN motif, cell behavior, re-epithelialization, wound healing, phospho-FAK-Tyr397, Rac1-GTP, rat excisional wound splinting model

Student Number: 2015-22086

CONTENTS

LIST OF FIGURES

BACKGROUND

Skin and wound

The skin is a highly specialized tissue that defenses against water loss, excludes toxins, and resists mechanical stress, and also it is a highly developed immune system itself. Mammalian skin consists of multiple layers *e.g.*, epidermis, dermis, and hypodermis (1). The epidermis is the superficial layer of skin which is composed of keratinocytes, with a small proportion of Langerhans cell and melanocyte. Epidermis functions as a barrier of our body, which protects unwelcomed invasions and conserves body moisture (2). The underlying dermis is a connective tissue supporting epidermis. There are a number of vessels in dermis, and its extracellular matrix (ECM) contains type I collagen and elastin, which are suitable for mechanical stimuli. The hypodermis, which also functions as the endocrine system, is a loose connective tissue that binds the skin to underlying organs. It functions for cushioning, energy storing and heat-regulating by reason of its fats and adipocytes. The hypodermis is not only a fat storing tissue, but also a complex reservoir of stem cells, hormones, and growth factors (1, 2).

The skin functions as a protective barrier against surroundings. Severe injury or illness of skin can result in major disability or even death by reason of body moisture leakage and pathogen invasion into our body (3). Wound healing can be affected by local factors like oxygenation (4, 5) and infections (6, 7), and by several systemic factors such as age (8, 9), sex hormones (10, 11), stress (12, 13), diabetes (14, 15), medications (16-18), obesity (19, 20), alcohol consumption (21, 22), smoking (23, 24), and nutrition (25, 26).

In the moment after an injury occurs, myriads of pathways are activated for tissue homeostasis. Additionally, the immune system accompanying inflammation and the blood coagulation cascade are activated after skin injury. Many types of cells including immune cells, endothelial cells, keratinocytes, and fibroblasts proliferate and differentiate to recover tissue injury (27, 28). In this regard, keratinocytes and fibroblasts are mainly considered in this study, which aims for accelerating *in vivo* wound healing procedure with a peptide.

Wound healing procedure

Wound healing occurs through overlapping several phases; hemostasis, inflammation, proliferation, and remodeling (27-29). The general wound healing procedure is described in Fig. 1. Immediately after a skin injury, the wound goes through the hemostasis stage, in which multiple physiologic responses are triggered to stop a hemorrhage. Coagulation is initiated by an aggregation of thrombocytes or platelets in a fibrin network, through the serial activation of tissue and plasma factors (30). Coagulation is needed not only for hemostasis but also for an organization of provisional matrix to which cells migrate, which eventually restores the skin's function as a protective barrier (31). Also, inflammatory cells are quickly recruited to the wound (29). Inflammatory cells release lysosomal enzymes and reactive oxygen species to scavenge various cell debris (32). Blood flow around the wound decreases by the constriction of local vascular smooth muscle cells. Soon, the wound area is covered by fibrin clot, in which various types of cells would infiltrate, including leukocytes, keratinocytes, and fibroblasts (28).

Tissue injury accompanies leakage of blood from vessels, which comes to be the

blood clot. This blood clot functions not only as a means of hemostasis but also as a temporary ECM. Activated platelets, parenchymal cells, and complements recruit inflammatory leukocytes to the site of injury (28, 31). During the inflammatory stage, neutrophils are recruited to the wound site to kill bacteria and to degrade damaged matrix protein. Monocytes follow after neutrophil and differentiate into macrophages to engulf microbes, break down the damaged matrix, and induce angiogenesis and tissue granulation (28, 33). These cells are responsible for wound inflammation, and they last for approximately two weeks unless the inflammation is prolonged, when wound tissue can go through severe chronic inflammation (34).

After scavenging foreign particles and bacteria by neutrophils and macrophages, the wound enters the proliferation stage or new tissue formation stage, which is characterized by the proliferation and migration of various parenchymal cells (33). Keratinocytes migrate from interfollicular epidermis into the injured area and undergo differentiation to rebuild the epidermal barrier, while various factors *e.g.*, growth factors, matrix metalloproteinases (MMPs), integrins, and structural proteins such as laminins, are involved (29). Along with the epidermal repair, new vessels are formed by multiple growth factors including vascular endotheial growth factor (VEGF) and fibroblast growth factor-2 (FGF-2). In concert with fibroblast and macrophage, capillaries replace fibrin clot to granulation tissue. At the end of this stage, fibroblasts differentiate into myofibroblasts to contract the wound edges (28, 33).

Once wounds reach to the remodeling stage, all procedures that occurred after the injury subside while newly formed ECMs replace old ones. Most of the endothelial cells, macrophages, and myofibroblasts go through apoptosis or leave the wound. Dermis

undergoes ECM remodeling in this period. For instance, type III collagen, which is the major collagen in the early time point of remodeling phase, is gradually replaced to type I collagen. Collagen remodeling is carried out by MMPs from fibroblasts, macrophages, and endothelial cells. The physical properties of wounded skin are improved during this remodeling phase, reaching around 40% of its original tensile strength at one month and up to 70% by one year. Unfortunately, wounds never reach the same breaking strength (the tension at which skin breaks) compared to the uninjured skin (28, 33).

Focusing on the early wound healing procedure, laminins, as the main components of the basement membrane, play significant roles by the reason that (re-)epithelization is indispensable to the existence of the basement membrane (35). In this context, laminin and its derivatives are considered as candidates for wound healing molecules in the current study.

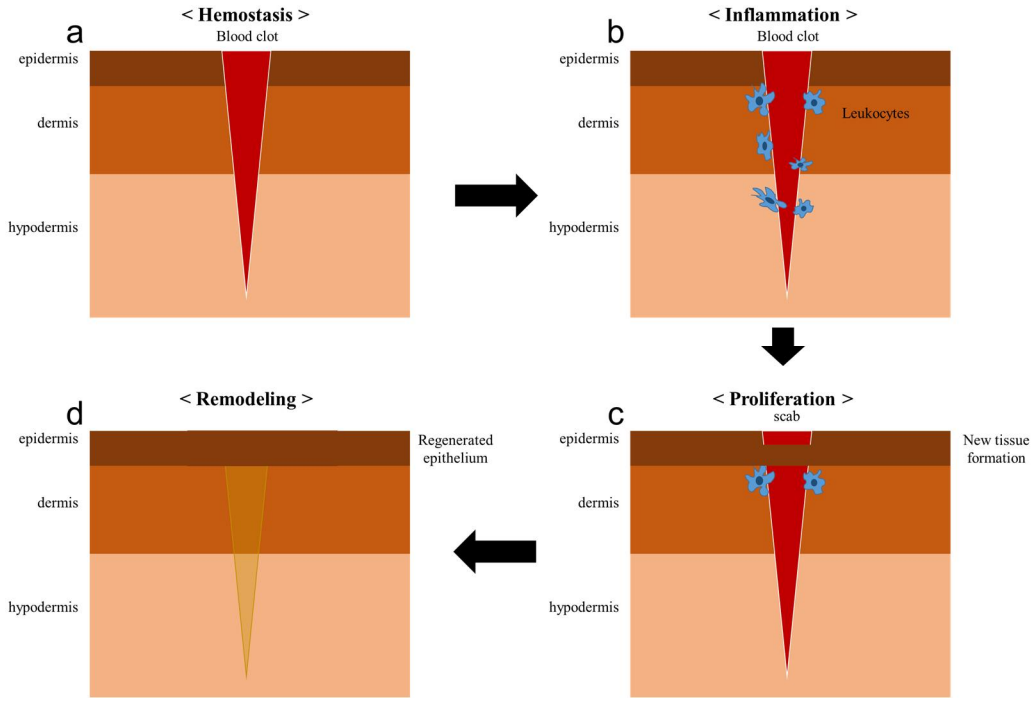

Figure 1. Wound healing procedure. a) While the hemostasis phase, coagulation occurs to seize bleeding from the injury and blood clot of the wound functions as the provisional matrix for recruited cells. b) inflammatory leukocytes are recruited to the wound site to scavenge foreign bacteria and damaged tissue matrix while promoting angiogenesis. c) after the inflammatory phase, parenchymal progenitor cells of vicinity migrate toward the wound to recover tissue integrity. In the case of the skin wound, keratinocytes, fibroblasts, and endothelial cells regenerate the epidermis, dermis, and vessels, respectively. d) when the repair of the wound tissue is accomplished in some extents, the recruited leukocytes and endothelial cells diminishes and the composition of the dermal ECM is altered through years.

Laminin structure

Laminins are one of the major components of the basement membranes which are heterotrimeric proteins with combination of one α, one β, and one γ chain (Fig. 2, left panel). In case of vertebrates, five α, three β, and three γ chains have been identified. Contrary to the expectation that there could be 45 laminin isoforms, merely 16 laminin isoforms have been identified (35). Even all these chains have common structural motifs, there are significant differences of α chain compared to the others (36). The α chain has a globular G domain consisting of five LG subdomains, which the β and γ chain do not have. Each LG subdomain consists of 14 β-strands (which are named as A to N strands) arranged in two sheets and loops connecting each β-strand, constructing roughly spherical structure with a diameter of approximately 3.5 nm (37). Next to the G domain, there is a long coiled-coil domain which is also in the β and γ chains to form the long arm of the laminin together. The N-termini of each chain are often called short arms and they are responsible for assembly among laminin proteins to be combined into the basement (36). The laminin proteins are assembled before secretion from the cell, but some laminin isoforms are modified by extracellular proteolytic processing at the N- or C-terminal ends before the laminin proteins reach their final forms (35, 36, 38).

Laminins show several biological effects such as adhesion, migration, differentiation of cells and key motifs related to the biological activities have been screened. The LN domain have responsibility for self-assembly to build the basement membranes (35), which can be called the “three-arm interaction model” of laminin polymerization (Fig. 2, right panel)(38). The coiled-coil domain is responsible for the triple α-helical coiled coil structure, while the five LG domains at the C-terminal end of a laminin interact to certain

receptors and some molecules of ECMs (35, 36, 38). These LG domains mainly bind to cellular integrin, dystroglycan, syndecan, sulfated glycolipids, and Lutheran blood group glycoprotein (35, 36) to promote various functions of cells such as adhesion, differentiation, migration, phenotype maintenance, and resistance to apoptosis. For example, the C-terminal LG domains of the laminin α2 chain bind to several integrin receptors, including α3β1, α6β1, α7β1, and α6β4 (39), and the N-terminal VI domain of the laminin α2 chain also has interacting sites for integrin receptors α1β1 and α2β1 (40). Laminins, not as common ECM proteins, but as components of the basement membrane, interact with cells through integrins, which is the main reason of the bioactivity of a laminin and its derivative employed in this study (41).

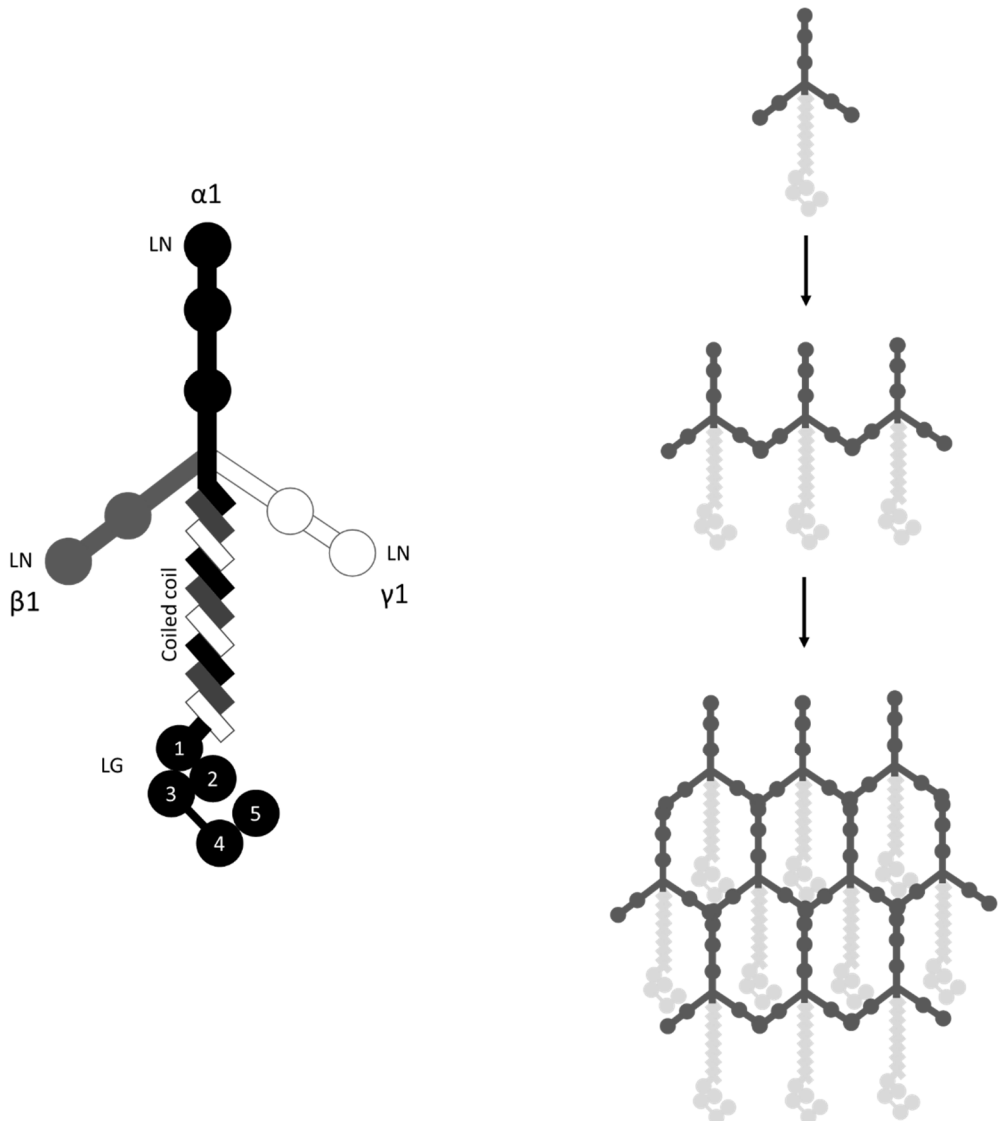

Figure 2. Structure of laminin 111 and scheme of laminin assembly. Laminins are heterotiimeric proteins composed of one, one β, and one γ subdomain (left panel). N-termini of each subdomain form "short arms" of the laminins, and these subdomains form a coiled-coil stem of the laminin. The α subdomain contains LG domains, which performs various bioactivities to cells. Laminins self-assemble mainly due to the LN domains of each subdomain, which is called "three-arm interaction model" (right panel).

Integrin signaling

Integrin protein is a transmembrane adhesive receptor that mediates mainly cell-ECM interactions (42). Integrin consists of one α subunit and one β subunit, and there are 24 different integrin heterodimers with the combination of 18 α subunits and 8 β subunits. Integrin is mainly related to cell adhesion and following intracellular signaling pathways, which is revealed to be closely related to several cellular functions *e.g.*, survival, proliferation, migration, and differentiation (42, 43). The general integrin activation and ECM binding of integrin are described in Fig. 3. Signals from cytoplasm can modulate the affinity of the integrin by unbending of the ligand-binding headpiece and conformational changes, leading to increased ligand-binding affinity ("inside-out" signaling; see Fig. 3.) (44, 45). On the contrary, the ligand-integrin binding provokes several intracellular signaling, which can be called "outside-in" signaling (Fig. 3) (42, 44, 45), and this signal is delivered to integrin binding partners *i.e.*, focal adhesion kinase (FAK), vinculin, talin, and paxillin (46), followed by activation of other downstream signaling molecules *e.g.*, mitogen-activated protein kinases (MAPKs) or Rho family GTPases (47). It is previously reported that laminin-211 derived peptide increase cell adhesion and spreading via integrin α3β1 and FAK in keratinocytes and fibroblasts (41).

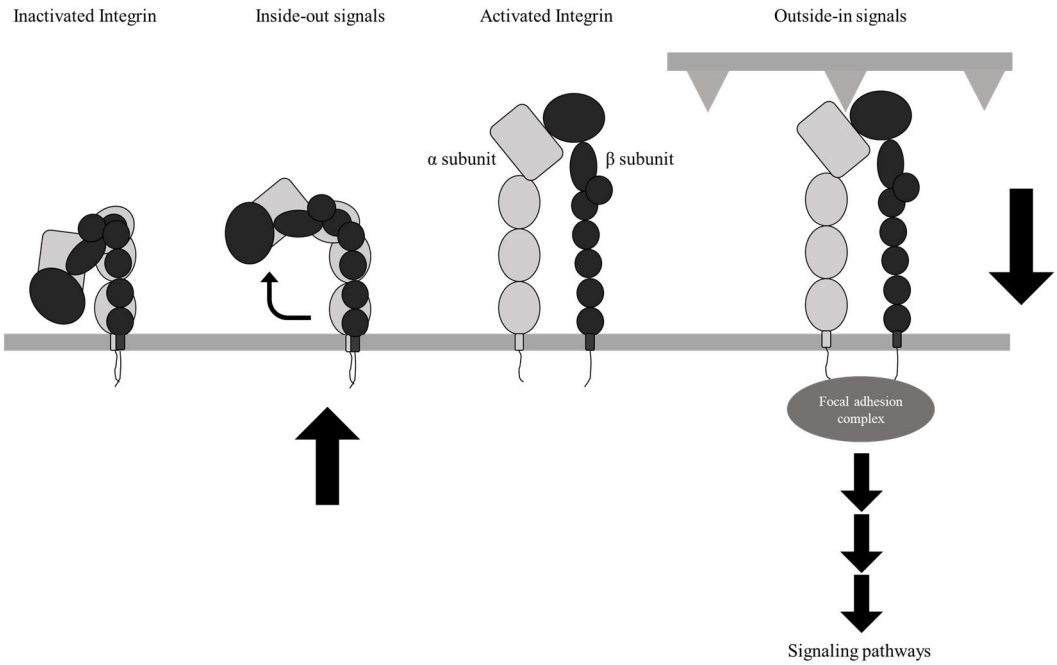

Figure 3. Inside-out and outside-in signals of integrins. Inactivated integrin shows low affinity to its ligands *e.g.*, ECM proteins or intercellular adhesion proteins, whereas some signals from cytoplasm (inside-out signals) can activate integrin resulting in improved integrin affinity to its ligands. Intracellular integrin partner proteins e.g., focal adhesion kinase (FAK), vinculin, talin, and paxillin, deliver the signals from ligand-bound integrins to the downstream signaling pathways to trigger several cellular behaviors (outside-in signals).

INTRODUCTION

Skin is the largest organ in our body and functions as a barrier against the intimidating invasion from the outer environment *e.g.*, toxins, bacteria, and mechanical stress. If skin continuity is broken by several events *e.g.*, surgery, trauma, and burn, patient's vitality will be seriously threatened (34, 48). When skin is damaged, the human body conducts serial processes to cover this discontinuity, which is called wound healing. Wound healing consists of four overlapping but distinct phases, which are hemostasis, inflammatory, new tissue formation or proliferation, remodeling phase respectively (27-29). In the moment after an injury occurs, myriads of pathways are activated for wound repair. Blood coagulation places first of this wound healing procedure. Coagulation is needed not only for hemostasis but also organization of provisional matrix for cell migration, which eventually restores the skin's function as a protective barrier (31). Next, the inflammatory pathway are activated and diverse cells such as immune cells, endothelial cells, keratinocytes, and fibroblasts cooperate to heal the injury (33). Keratinocytes migrate from interfollicular epidermis into the injured area and undergo differentiation to rebuild the epidermal barrier, while various factors e.g., growth factors, MMPs, integrins, and structural proteins such as laminins, are involved (29). Along with the epidermal repair, new vessels are formed by several growth factors *e.g.*, VEGF and FGF-2. In concert with fibroblast and macrophage, capillaries replace fibrin clot to granulation tissue. At the end of this stage, fibroblasts differentiate into myofibroblast to contract the wound edges (28, 33). After the proliferation stage, inflammation subsides and the old ECM is replaced to new ECM in the remodeling stage (33). It is evident that parenchymal cells *i.e.*,

keratinocyte and fibroblast, and ECM protein *i.e.*, laminin, play significant roles in the early wound healing procedure, by the reason that these cells are indispensable to the basement membrane, in which laminin is mainly involved (35).

Laminins are T-shaped heterotrimer glycoproteins found mainly in the basement membrane and affects various cellular functions such as proliferation, attachment, migration, and resistance to apoptosis, as well as the structural support of epithelium (35, 36, 38). Laminins consist of α, β, and γ chains and N-termini of each chain are related to self-organizing (35), depicted as “three-arm interaction model” (38). Next to the “short arm” of the N-termini, there is a long coiled-coil domain to form the “long arm” of the laminin. The α chain has different globular G domains at the C-terminal compared to the other chains, which are called LG domains. Each LG subdomain consists of 14 β-strands (which are named as A to N strands) arranged in two sheets and loops connecting each β-strand, constructing roughly spherical structure with a diameter of approximately 3.5 nm (37). It is known that the LG domains mainly bind to cellular integrins, dystroglycan, syndecan, sulfated glycolipids and Lutheran blood group glycoprotein (35, 36) to promote various functions of cells. Especially the LG domains are known to interact with integrin or syndecan to trigger intracellular signaling and cellular functions (39, 41, 49, 50). Indeed, the C-terminal LG domains bind to several integrin receptors, including α3β1, α6β1, α7β1, and α6β4 (39), and the N-terminal domain VI of the laminin α2 chain also has interacting sites for integrin α1β1 and α2β1 (40).

Bioactive peptide can be a new therapeutic substance by the reason that it may have an advantage over the protein itself (51). In order for a substance with regeneration ability to be used in clinical practice, it should be able to exert its original biological function

without triggering an immune response (52-54). For instance, recombinant human bone morphogenetic protein 2 (rhBMP2) is one of the growth factors showing an undesirable immune response, which exhibits an inflammatory and osteolytic effect, despite its excellent effect of bone regeneration (55, 56). In contrary, it is generally thought that peptides with length under 12 amino acids are not recognized by class II MHC receptors, which is one of the key molecules of $CD4^+$ T lymphocytes in immune recognition (57). The simple and economical production of peptides compared to proteins means that they are comparable to protein therapeutics such as antibodies or growth materials in terms of drug targeting, efficacy, stability, and bioavailability (51, 58-60). With this regard, various peptides are being studied and developed for clinical use (60). The motif RNIPPFEGCIWN (amino acids 2675−2686; Ln2-LG3-P2) is already reported to be effective in cell adhesion, spreading, and migration via integrin α3β1 and FAK (41), and motif PPFEGCIWN (amino acids 2678−2686, Ln2-LG3-P2-DN3) is revealed to have a bone regeneration capacity (50). In this study, it is hypothesized that the PPFEGCIWN motif would accelerate wound healing without detrimental inflammation. The effects of this laminin-derived peptide toward adhesion and spreading capacity of keratinocytes and fibroblasts were verified, which are closely related cell behaviors in the wound healing *in vivo*. Next, inflammatory reaction between this peptide and rats was identified in the context of the biocompatibility. Finally, the wound healing capacity of this peptide in rodent model and accompanying expression of related proteins were evaluated.

MATERIALS AND METHODS

Animals and materials

Eight-week-old male Sprague-Dawley rats were purchased from Orient BIO Inc. (Seongnam, Korea). All the experimental methods are approved by the Seoul National University Animal Experiment Committee. The peptides were synthesized by the C-terminal amide Fmoc (9-fluorenylmethoxycarbonyl)-based solid-phase method with Pioneer peptide synthesizer by Peptron (Daejeon, Korea). Peptides over 95% purity as determined by high-performance liquid chromatography (HPLC) were used in this experiment. Human placental laminin was purchased from Sigma Aldrich (St. Louis, MO, the United States). Beschitin W, a commercial nonwoven-type chitin microfiber matrix, was purchased from Unitika Co. (Osaka, Japan).

Culture of primary cells

Normal human epithelial keratinocytes (NHEKs) and normal human dermal fibroblasts (NHDFs) were isolated from human foreskins obtained from patients (1-3 years of age) undergoing surgery. Excised foreskins were washed in calcium- and magnesium-free Hanks' balanced salt solution (HBSS). The epidermal layer is separated from the underlying dermis by incubation in HBSS containing collagenase (type II; 1.0 mg/ml, Sigma, St. Louis, MO, the United States) and dispase (grade II; 2.4 mg/ml, Boehringer-Mannheim. Indianapolis, IN, the United States) for 90 min at 37 °C in an atmosphere of 95% air and 5% CO_2. Epidermal keratinocytes were then isolated from separated epithelial

tissue by trypsinization in 37 °C for 4 min, and primary cultures were established in keratinocyte growth medium containing 0.15 mM calcium and a supplementary growth-factor bullet kit (KGM; Clonetics, San Diego, CA, the United States) with a plating of 2×10^5 cells in 60-mm cell culture dish. The second passage cells with lower population doublings were used in the described experiments. The NHDFs were established from the explant culture of the abovementioned foreskin dermis. The remained dermal tissues were physically chopped and laid on the 100-mm culture dish with attachment. After a week, cells that migrate and proliferate from the explant culture were continuously cultured in Dulbecco's modified Eagle's medium (DMEM) supplemented with 10 % fetal bovine serum (FBS) and 1 % penicillin-streptomycin. The cells in their fourth passage were used for several assays. All procedures of sampling human tissue specimens were in accordance with the guidelines of the Institutional Review Board on Human Subjects Research and Ethics Committee at Seoul National University Dental Hospital, Seoul, Korea.

Immobilization of synthetic peptides

Twenty-four-well plates (Nunc, Roskilde, Denmark) were coated with synthetic peptides (13.1 μg/cm^2) by drying for 12 hr at room temperature or with laminin (1 μg/ml) by applying it for 12 hr at 4 °C and then washed with phosphate-buffered saline (PBS). Beschitin W matrices were cut out with a 14 mm-diameter punch and placed in 24-well culture plates. These chitin microfiber matrices were coated with peptides or laminin in the same way of plate coating and then washed with PBS. The coated plates were blocked with 1 % heat-inactivated bovine serum albumin (BSA) for 1 hr at 37 °C and then washed twice with PBS.

Cell adhesion and spreading assays

For adhesion and spreading assay, 1×10^5 cells were placed in each 24-well plates or matrices coated in aforementioned conditions with BSA, laminin, or synthetic peptide, and were allowed to adhere for 1 hr or 3 hr to verify its adhesion or spreading aspects respectively, at 37 °C in 5 % CO_2 (n = 5). The wells were washed once with PBS, and the remaining bound cells were fixed with 10 % formalin in PBS for 15 min. The fixative was aspirated; the wells were washed twice with PBS, and attached cells of the culture plates and chitin microfiber matrices were stained with 0.5 % crystal violet solution. The wells for adhesion were gently washed 3 times with double-distilled water (DDW). Each plate sample was divided into quarters and two fields per each quarter were photographed with an Olympus BX51 microscope at 100×. For the plate-adhesion sample, the contents of each well were solubilized in 2 % sodium dodecyl sulfate (SDS) for 5 min. The intensity of the crystal violet staining was measured at 570 nm with a microplate reader (Bio-Rad, Hercules, CA, the United States). For the spreading assay, the relative area of spread cells in the image file was measured with Image-Pro Plus software (Media Cybernetics, Bethesda, MD, the United States). The chitin microfiber matrices were mounted on the slide glasses, and cells attached to the microfibers were photographed. They were photographed in the same way as the plate sample with a Leica DM5000B microscope at 100×. Cells were counted to quantify the degree of adhesion. The cells with a flattened, polygonal shape, which shows filopodia- and lamellipodia-like extensions, were regarded as spread cells. In contrast, the cells that merely attached to the plate or the microfiber surface without a polygonal shape were regarded as non-spread cells. The spread sample

of microfiber was quantified in the same way as the plate-spread sample's method.

Histological examination of the rat skin inflammation with Ln2-LG3-P2-DN3 peptide

The subcutaneous inflammatory reaction caused by the peptide was observed in 8-week-old male rats. After anesthetizing the rat and shaving the dorsum, an incision of 1 to 2 cm was made along the midline on the dorsum. After gently freeing the subcutaneous tissue from the underlying muscle on each side, the Beschitin W matrices treated with the vehicle or Ln2-LG3-P2-DN3 peptide were embedded subcutaneously under the incision (n = 4). The Beschitin W matrix was prepared as 8 × 8 mm pieces and coated. After the matrices were placed on a 100 mm Petri dish, vehicle (DMSO) and synthetic peptide (1 mg/cm^2) were applied on matrices and dry-coated at room temperature for 12 hr. The incision was closed with three simple interrupted sutures by 4-0 Dafilon (Braun Surgical, Rubi, Spain). Three days after the operation, all rats were sacrificed and the dorsum skins were harvested, fixed, paraffin-embedded, sectioned, and stained with hematoxylin and eosin (H&E). After staining, Tissue sections were photographed on a Leica DM5000B microscope. On the image, 15 squares of 150 × 150 μm were defined in the space around the matrix and in the space within the matrix respectively to count the pro-inflammatory cells in the space.

Determination of re-epithelialization in the skin wounds of Ln2-LG3-P2-DN3-treated rats

From 8-week-old male rats, the degree of wound healing and re-epithelization of the wound treated with peptides were measured. All rats were shaved with electric clippers and hair removal cream the day before the surgery. Six wounds were formed on the dorsum of 12 rats, each 5 mm in diameter. The rats were divided into 3 groups, which assign to days 1, 2, and 3 respectively. A Beschitin W matrix with a diameter of 8 mm was placed on a culture plate and each vehicle (50 % DMSO dissolved in DDW) or synthetic peptide (1 mg/cm^2) was applied. The matrices were dried at room temperature for 12 hr to be coated. The matrix was then placed on each wound of the rats and fixed around the wound with cyanoacrylate adhesive and silicone ring. The silicone rings were prepared with an outer diameter of 15 mm, an inner diameter of 6 mm, and a thickness of 1 mm. After placing the ring, each ring was sutured with a 4-0 Dafilon. Wound images were taken immediately after surgery on days 1, 2, and 3, and the area of the wound was measured with Image-J software (National Institutes of Health, Bethesda, MD, the United States). The wounded tissues were harvested after 1, 2, and 3 days postoperatively, fixed, paraffin-embedded, and sectioned to be stained with H&E. For representative observations, each wounded tissue was cut symmetrically in the center of the wound for tissue sections. Each length of the re-epithelialized tissue was determined on the image. All animal procedures were reviewed and approved by the animal care committee of the Institute of Laboratory Animal Resources of Seoul National University (approval number: SNU-151209-2-1).

Immunohistochemisty of skin wound with Ln2-LG3-P2-DN3-related intracellular signaling molecules

In situ expression of phospho-FAK-Tyr397 and active Rac1 were determined in tissue specimens by immunohistochemistry. The rat skin wound tissues were embedded in the paraffin blocks and prepared for tissue section slides. Using the Discovery XT automated immunohistochemistry stainer (Ventana Medical Systems Inc., Tucson, AZ, the United States), slides were stained as the following procedure: Sections were deparaffinized using the EZ Prep solution, then CC1 standard (pH 8.4 buffer contained Tris/Borate/EDTA) and inhibitor D (3 % H2O2, Endogenous peroxidase) were used for antigen retrieval and blocking for 4 min at 37 °C temperature, respectively. Slides were incubated with primary antibodies for 32 min at 37 °C, and Omimap secondary antibodies for 20 min at 37 °C. After the treatment of antibodies, slides were incubated in diaminobenzidine (DAB) with an H_2O_2 substrate for 8 min at 37 °C followed by hematoxylin and bluing reagent counterstain at 37 °C. Reaction buffer (pH 7.6 Tris buffer) was used as a washing solution. Detection was done using the Ventana DAB Map Kit (Ventana Medical Systems Inc., Tucson, AZ, the United States). Primary antibodies of anti-phospho-FAK-Tyr397 antibody (1:200, 44-624G, Thermofisher Scientific, Rockford, IL, the United States) and anti-active Rac 1 antibody (1:1000, 26903, NewEast, King of Prussia, PA, the United States) were used for these experiments. Only the extension of the epithelialization of day 3 slide images, from the wound edge to the epithelialized margin, were digitally cropped. The staining intensity of each cropped image the was quantified with densitometric analysis using the plugin named as IHC profiler (https://sourceforge.net/projects/ihcprofiler/) of Image-J software.

Statistical analysis

Statistical analysis of data was performed using the STATISTICA 6.0 software package. The results were compared by an analysis of variance (ANOVA). When significant differences were found, post-hoc adjustments were performed using a Scheffe's adjustment. The two group comparison was performed using the Student's t-test. P-values less than 0.05 were considered significant.

RESULTS

Effects of Ln2-LG3-P2-DN3 on cell behavior of normal human cells

By the reason that the cell behaviors *e.g.*, adhesion and spreading, are closely related to skin regeneration (61, 62), adhesion and spreading assays were conducted to determine the effect of laminin-derived Ln2-LG3-P2-DN3 peptide on NHEKs and NHDFs *in vitro*. Cells were placed in a culture dish coated with laminin, BSA, scrambled peptide (SP), or Ln2-LG3-P2-DN3 peptide, and the attachment and spreading of the cells are identified (Fig. 4). When incubated for 1 hr for adhesion assay, both NHEKs and NHDFs showed a typical *in vitro* morphology on plates, while little NHDFs attached to the BSA- and SP-coated plates (Fig. 4 and Fig. 5). Both NHEKs and NHDFs showed high adhesion to the Ln2-LG3-P2-DN3-coated plates. When incubated under the same conditions for 3 hr, both NHEKs and NHDFs showed higher cell adhesion aspect and clearer spreading pattern on the bare culture dish (Polystyrene, PS), laminin-coated, and LN2-LG3-P2-DN3-coated plate, while NHDFs did not spread well and showed aggregated pattern on the BSA- and SP-coated plates (Fig. 6 and Fig. 7). In the case of NHEKs, the degree of spreading did not show a clear difference between the groups, while Ln2-LG3-P2-DN3- and laminin-treated groups of NHDFs showed prominent spread patterns. Combined together, Ln2-LG3-P2-DN3 peptide showed a considerable capacity of adhesion and spreading to laminin in both NHEKs and NHDFs, which suggests that this peptide still contains the bioactivity of laminin with strikingly compact molecular size (9-mer peptide) compared to proteins.

The adhesion and spreading of NHEKs and NHDFs on peptide-coated chitin microfibers were further investigated. Chitin is a widely distributed polysaccharide in nature known to have a wound-healing effect (63, 64), and there are many chitin commercials as wound dressings. NHEKs and NHDFs were placed in a chitin matrix each coated with laminin, BSA, scrambled peptides, or Ln2-LG3-P2-DN3 peptides, and their adhesion and spreading were observed (Fig. 8 to 11). In adhesion assay, a larger number of cells were attached to the laminin- or Ln2-LG3-P2-DN3- coated matrices compared to the other matrices. NHEKs adhered to the bare matrix in a certain extent, while little NHDFs adhered to the bare matrix, similar to BSA (Fig. 8 and Fig. 9). In the case of the spreading assay in the same condition, NHEKs showed more spreading aspects on the Ln2-LG3-P2-DN3-coated matrix than laminin- or SP- coated ones (Fig. 10). NHDFs showed a more spreading tendency on the Ln2-LG3-P2-DN3-coated matrix than SP- coated one (Fig. 11). Taken together, this Ln2-LG3-P2-DN3 peptide presented bioactivities *i.e.*, adhesion and spreading, toward both NHEKs and NHDFs even coated on chitin matrix, which implies the possibility that this peptide can be applied to the several *in vivo* lesions with chitin microfiber scaffolds

Histological evaluation of inflammatory response to Ln2-LG3-P2-DN3 in vivo

Biocompatibility is one of the important aspects of biomaterials for tissue regeneration, as excessive inflammation can inhibit tissue regeneration or cause rejection when biomaterials are applied (54, 65). In this regard, the inflammatory response with

Ln2-LG3-P2-DN3 peptide in rats was examined. Vehicle and Ln2-LG3-P2-DN3 peptide were employed to coat the Beschitin W matrix respectively, and these coated matrices were placed in the dorsal subcutaneous region of the rats for 3 days. Pro-inflammatory cells which are recruited in the matrix and in the tissue near the matrix (Fig. 12) were counted to identify the difference between vehicle and peptide. The inflammatory response in and around the matrix was not significantly different between the vehicle and Ln2-LG3-P2-DN3-coated matrices. Consistently, there was no extension of inflammation around the matrix, and all surrounding tissues showed normal histological features. Ln2-LG3-P2-DN3 peptide caused no detrimental inflammation *in vivo*.

Effects of Ln2-LG3-P2-DN3 on early-stage cutaneous wound healing

Based on the observation that Ln2-LG3-P2-DN3 peptide is effective for adhesion and spreading of keratinocytes and fibroblasts *in vitro*, the early wound healing effects of Ln2-LG3-P2-DN3 peptide on the skin of rats were examined. After the formation of full-thickness round-shaped wounds on the dorsum skin of rats, chitin matrices coated with vehicle or synthetic peptide were mounted, and wounds on days 1, 2, and 3 were visually observed. The overall size of the wounds was found to decrease along with time (Fig. 13), and the Ln2-LG3-P2-DN3-treated wounds were smaller compared to the other ones in the same day. In addition, wound tissues were harvested to make tissue sections, which were stained with H&E to determine the area of re-epithelialization (Fig. 14). On days 1 and 2, there was no significant difference between the groups, while the Ln2-LG3-P2-DN3-

treated group showed a significant increase in extension of epithelialization on day 3, compared with the other groups.

Promotion of FAK-Tyr397 phosphorylation and Rac1 activation during early cutaneous wound healing

The Ln2-LG3-P2 peptide is already reported to interact with cells via integrin α3β1 and Phospho-FAK-Tyr397 (41). To confirm these phenomena *in vivo*, immunohistochemical analysis with an anti-phospho-FAK-Tyr397 antibody was conducted with the vehicle or peptide-treated day 3 wounds (Fig. 15). Phospho-FAK-Tyr397 is distributed along with the re-epithelized area, and the intensity showed an increasing tendency in the Ln2-LG3-P2-DN3-treated wound compared to vehicle or SP-treated wounds. Next, active Rac1 was also quantified in the same way as phosphor-FAK-Tyr397 in vehicle or peptide-treated day 3 wounds (Fig. 16). The Ln2-LG3-P2-DN3-treated wound showed significantly increased active Rac1 intensity compared to vehicle or SP-treated wounds. These data are consistent to the above-mentioned reports (41) and it implies that the *in vivo* early wound healing effect of the Ln2-LG3-P2-DN3 peptide is due to the intracellular signaling including integrin α3β1, phospho-FAK-Tyr397, and active Rac1.

DISCUSSION

In this study, the abovementioned serial experiments were conducted to investigate whether the peptide has potentials as a therapeutic substance. The recovery of the wound occurs when various cells such as immune cells, endothelial cells, keratinocytes, and fibroblasts exert their phenotype of proliferation, differentiation, and migration (33, 66). After covering the wound lesion, keratinocytes and fibroblasts secrete ECM to fuse with a new basement membrane (67). The Ln2-LG3-P2-DN3 peptide promoted adhesion and spreading of human keratinocytes and fibroblasts in both culture dishes and matrices. Since early cell adhesion and spreading are important in wound healing (61, 62, 68), the results that Ln2-LG3-P2-DN3 peptide promoted cellular responses of NHEKs and NHDFs, typical cells involved in wound healing, suggest this peptide can contribute to improving wound healing procedure.

To date, Ln2-LG3-P2-DN3 is the only active site that has a biological function in the LG3 domain of the laminin α2 chain (50). The LG3 domain of the laminin α2 chain is composed of 14 β-sheet strands labeled A through N, connected with loops (37), and Ln2-LG3-P2-DN3 is located in the loop between the K and L strands (41). It is partly consistent with the previous report that GD-6 peptide (KQNCLSSRASFRGCVRNLRLSR, amino acids 3011−3032), which is a functional motif located in the K-L loop of the C-terminal LG5 domain of murine laminin α1, interacts with integrin α3β1 to enhance keratinocyte adhesion (69). Also, as noted in previous reports, the peptides with these 9 residues showed a biological effect corresponding to the activity of the laminin in this experiment, while not having any secondary structure.

Inflammation is an indispensable process in wound healing, not only as a defense system toward the microorganisms but also as a recruiting system for various regenerating cells. However, excessive inflammation can result in reduced restoration or rejection (54, 65), suggesting that the wound restorative material should also be biocompatible without causing detrimental inflammation. To confirm the biocompatibility of the peptide, the peptide-coated chitin matrices were inserted subcutaneously in rats to see if the Ln2-LG3-P2-DN3 peptide would cause an excessive inflammatory response *in vivo*. The histology data revealed that there was no significant difference in inflammation between the peptide-treated chitin matrix and vehicle. In other words, there was little inflammatory reaction caused only by the peptide itself, and it is consistent with the aforementioned statement that peptides with length under 12 amino acids are not considered immunogenic (57), which is its advantage in the issue of tissue engineering. Based on these data, it is confirmed that this Ln2-LG3-P2-DN3 peptide is biocompatible enough to be adjusted toward the *in vivo* system.

It was evident that Ln2-LG3-P2-DN3 peptide accelerated the early wound healing in a rat wound model in current study. Unlike human skin, the skin of the rat is not fixed to the underlying tissues, which results in prominent wound contraction and significant postural wound deformation (70). Silicone splints were used to mimic the character of a human wound on the skin of the rat. After the wound forming operation, rats were allowed to recover for 1, 2, and 3 days, respectively. The Ln2-LG3-P2-DN3 peptide was found to accelerate the initial wound healing while the wound contraction was excluded. This result was also confirmed by the histology data that the re-epithelialized portion of the Ln2-LG3-P2-DN3-treated groups was significantly larger than that of the vehicle or SP-treated ones.

Next, immunohistochemical analyses were conducted to identify the expression of phospho-FAK-Tyr397 and active Rac1 in the rat wounds. Phospho-FAK-Tyr397 and active Rac1 were expressed along with the epithelial extension and they showed increased expression in the Ln2-LG3-P2-DN3-treated wound. These results are in accordance with the previous report that the Ln2-LG3-P2 peptide interacts with cells via integrin α3β1 and phospho-FAK-Tyr397 (41). Unfortunately, the quantified intensity of phospho-FAK-Tyr397 did not show statistically significant differences between groups (P-value = 0.1 ~ 0.3). It might be due to the complex composition of tissues and organs, where myriads of cells communicate and interact with one another. There would be another possibility that the phosphorylation of FAK, the up-stream protein of the integrin-mediated signaling cascade, had been already ameliorated, based on a previous report that the expression level of phospho-FAK-Tyr397 is reduced only after 1 hr of laminin treatment or Ln2-LG3-P2 peptide treatment *in vitro* (41). Fortunately, activation of Rac1 in the Ln2-LG3-P2-DN3-treated groups were significantly improved compared to the other groups *in vivo*.

As considering that the Ln2-LG3-P2-DN3 peptide promotes osteoblast differentiation and regeneration of damaged bone tissue (50), it is possible that laminin may affect the recovery of other tissues and that laminin derived peptides are likely to have potentials to be widely used in tissue engineering. In addition to this study, several studies such as investigating other application methods of the Ln2-LG3-P2-DN3 peptides, the action of the Ln2-LG3-P2-DN3 peptide in late wound healing, and the effect of the Ln2-LG3-P2-DN3 peptide on other tissues will need to be studied further.

In summary, the effects of the PPFEGCIWN motif of human laminin α2 chain were investigated on *in vitro* keratinocyte and fibroblast culture system and *in vivo* rat wound

model. For the *in vitro* study, the Ln2-LG3-P2-DN3 peptide-coated dish and the chitin matrix promoted adhesion and spreading of the cells. In the subcutaneous area treated with Ln2-LG3-P2-DN3, only minimal infiltration of inflammatory cells was observed in the embedded matrix and the vicinity. In wound healing experiments *in vivo*, Ln2-LG3-P2-DN3-coated matrices applied to the full thickness wounds of rats accelerated the initial wound healing and re-epithelization. Ln2-LG3-P2-DN3 peptide up-regulated the phospho-FAK-Tyr397 and active Rac1 level of the wound epithelial tissue. The Ln2-LG3-P2-DN3 peptide is concluded to be a good candidate for biomedical treatment for skin wounds, as revealed both *in vitro* and *in vivo*.

REFERENCE

1. Yu, J.R., et al., Current and Future Perspectives on Skin Tissue Engineering: Key Features of Biomedical Research, Translational Assessment, and Clinical Application. Adv Healthc Mater, 2019. **8**(5): p. e1801471.
2. Farage, M.A., et al., Structural characteristics of the aging skin: a review. Cutan Ocul Toxicol, 2007. **26**(4): p. 343-57.
3. Singer, A.J. and R.A.F. Clark, Cutaneous Wound Healing. New Engl J Med, 1999. **341**: p. 738-46.
4. Bishop, A., Role of oxygen in wound healing. J Wound Care, 2008. **17**: p. 3969-402.
5. Rodriguez, P.G., et al., The role of oxygen in wound healing: a review of the literature. Dermatol Surg, 2008. **34**(9): p. 1159-69.
6. Edwards, R. and K. Harding, Bacteria and wound healing. Curr Opin Infect Dis, 2004. **17**(2): p. 91-6.
7. Menke, N.B., et al., Impaired wound healing. Clin Dermatol, 2007. **25**(1): p. 19-25.
8. Gosain, A. and L.A. DiPietro, Aging and wound healing. World J Surg, 2004. **28**(3): p. 321-6.
9. Keylock, K.T., et al., Exercise accelerates cutaneous wound healing and decreases wound inflammation in aged mice. Am J Physiol Regul Integr Comp Physiol, 2008. **294**(1): p. R179-84.
10. Gilliver, S.C., J.J. Ashworth, and G.S. Ashcroft, The hormonal regulation of

cutaneous wound healing. Clin Dermatol, 2007. **25**(1): p. 56-62.

11. Hardman, M.J. and G.S. Ashcroft, Estrogen, not intrinsic aging, is the major regulator of delayed human wound healing in the elderly. Genome Biol, 2008. **9**: p. R80.

12. Boyapati, L. and H.L. Wang, The role of stress in periodontal disease and wound healing. Periodontol 2000, 2007. **44**: p. 195-210.

13. Godbout, J.P. and R. Glaser, Stress-induced immune dysregulation: implications for wound healing, infectious disease and cancer. J Neuroimmune Pharmacol, 2006. **1**(4): p. 421-7.

14. Brem, H. and M. Tomic-Canic, Cellular and molecular basis of wound healing in diabetes. J Clin Invest, 2007. **117**(5): p. 1219-22.

15. Vincent, A.M., et al., Oxidative stress in the pathogenesis of diabetic neuropathy. Endocr Rev, 2004. **25**(4): p. 612-28.

16. Wagner, A.E., et al., Dexamethasone impairs hypoxia-inducible factor-1 function. Biochem Biophys Res Commun, 2008. **372**(2): p. 336-40.

17. Krischak, G.D., et al., The effects of non-steroidal anti-inflammatory drug application on incisional wound healing in rats. J Wound Care, 2007. **16**: p. 76-8.

18. Franz, M.G., D.L. Steed, and M.C. Robson, Optimizing healing of the acute wound by minimizing complications. Curr Probl Surg, 2007. **44**(11): p. 691-763.

19. Wilson, J. and J. Clark, Obesity: Impediment to Postsurgical Wound Healing. Adv Skin Wound Care, 2004. **17**: p. 426-32.

20. Momeni, A., et al., Complications in abdominoplasty: a risk factor analysis. J Plast Reconstr Aesthet Surg, 2009. **62**(10): p. 1250-4.

21. LM, G., et al., Acute ethanol intoxication increases the risk of infection following penetrating abdominal trauma. J Traum, 1993. **34**: p. 669-74.

22. Szabo, G. and P. Mandrekar, A recent perspective on alcohol, immunity, and host defense. Alcohol Clin Exp Res, 2009. **33**(2): p. 220-32.

23. Jensen, J.A., et al., Cigarette Smoking Decreases Tissue Oxygen. Arch Surg, 1991. **126**: p. 1131-4.

24. Ahn, C., P. Mulligan, and R.S. Salcido, Smoking-the Bane of Wound Healing: Biomedical Interventions and Social Influences. Adv Skin Wound Care, 2008. **12**: p. 227-36.

25. Campos, A.C.L., A.K. Groth, and A.B. Branco, Assessment and nutritional aspects of wound healing. Curr Opin Clin Nutr, 2008. **11**: p. 281-8.

26. H, H., et al., Benefits of an oral nutritional supplement on pressure ulcer healing in long-term care. J Wound Care, 2008. **17**: p. 476-8.

27. Eming, S.A., T. Krieg, and J.M. Davidson, Inflammation in wound repair: molecular and cellular mechanisms. J Invest Dermatol, 2007. **127**(3): p. 514-25.

28. Sun, B.K., Z. Siprashvili, and P.A. Khavari, Advances in skin grafting and treatment of cutaneous wounds. Science, 2014. **346**(6212): p. 941-5.

29. Falanga, V., Wound healing and its impairment in the diabetic foot. Lancet, 2005. **366**(9498): p. 1736-43.

30. Martin, P., Wound healing-Aiming for perfect skin regeneration. Science, 1997. **276**: p. 75-81.

31. Shaw, T.J. and P. Martin, Wound repair at a glance. J Cell Sci, 2009. **122**(Pt 18): p. 3209-13.

32. Medrado, A.R., et al., Influence of low level laser therapy on wound healing and its biological action upon myofibroblasts. Lasers Surg Med, 2003. **32**(3): p. 239-44.

33. Gurtner, G.C., et al., Wound repair and regeneration. Nature, 2008. **453**(7193): p. 314-21.

34. Dreifke, M.B., A.A. Jayasuriya, and A.C. Jayasuriya, Current wound healing procedures and potential care. Mater Sci Eng C Mater Biol Appl, 2015. **48**: p. 651-62.

35. Durbeej, M., Laminins. Cell Tissue Res, 2010. **339**(1): p. 259-68.

36. Domogatskaya, A., S. Rodin, and K. Tryggvason, Functional diversity of laminins. Annu Rev Cell Dev Biol, 2012. **28**: p. 523-53.

37. Timpl, R., et al., Structure and function of laminin LG modules. Matrix Biol, 2000. **19**: p. 309-17.

38. Hohenester, E. and P.D. Yurchenco, Laminins in basement membrane assembly. Cell Adh Migr, 2013. **7**(1): p. 56-63.

39. Suzuki, N., F. Yokoyama, and M. Nomizu, Functional sites in the laminin alpha chains. Connect Tissue Res, 2005. **46**(3): p. 142-52.

40. Colognato, H., et al., The Laminin α2-Chain Short Arm Mediates Cell Adhesion through Both the α1β1 and α2β1 Integrins. J Biol Chem, 1997. **272**: p. 29330-6.

41. Jung, S.Y., et al., The potential of laminin-2-biomimetic short peptide to promote cell adhesion, spreading and migration by inducing membrane recruitment and phosphorylation of PKCdelta. Biomaterials, 2012. **33**(15): p. 3967-79.

42. Barczyk, M., S. Carracedo, and D. Gullberg, Integrins. Cell Tissue Res, 2010. **339**:

p. 269-80.

43. Clark, E.A. and J.S. Brugget, Integrins and Signal Transduction Pathways: The Road Taken. Science, 1995. **268**: p. 233-9.

44. MA, S., S. MD, and G. MH, INTEGRINS: Emerging Paradigms of Signal Transduction. Annu Rev Cell Dev Biol, 1995. **11**: p. 549-99.

45. Askari, J.A., et al., Linking integrin conformation to function. J Cell Sci, 2009. **122**(Pt 2): p. 165-70.

46. Liu, S., D.A. Calderwood, and M.H. Ginsberg, Integrin cytoplasmic domain-binding proteins. J Cell Sci, 2000. **113**: p. 3563-71.

47. Schlaepfer, D.D. and T. Hunter, Integrin signalling and tyrosine phosphorylation: just the FAKs? Trends Cell Biol, 1998. **8**: p. 151-7.

48. Blais, M., et al., Concise review: tissue-engineered skin and nerve regeneration in burn treatment. Stem Cells Transl Med, 2013. **2**(7): p. 545-51.

49. Jung, S.Y., et al., A biologically active sequence of the laminin alpha2 large globular 1 domain promotes cell adhesion through syndecan-1 by inducing phosphorylation and membrane localization of protein kinase Cdelta. J Biol Chem, 2009. **284**(46): p. 31764-75.

50. Yeo, I.S., et al., Identification of a bioactive core sequence from human laminin and its applicability to tissue engineering. Biomaterials, 2015. **73**: p. 96-109.

51. Lee, J.-Y., et al., Bioactive Peptide-modified Biomaterials for Bone Regeneration. Curr Pharm Design, 2011. **17**: p. 2663-76.

52. Langer, R. and J.P. Vacanti, Tissue engineering. Science, 1993. **260**: p. 920-6.

53. Griffith, L.G. and G. Naughton, Tissue Engineering-Current Challanges and

Expanding Opportunities. Science, 2002. **295**: p. 1009-14.

54. O'Brien, F.J., Biomaterials & scaffolds for tissue engineering. Mater Today, 2011. **14**(3): p. 88-95.

55. Baldo, B.A., Side effects of cytokines approved for therapy. Drug Saf, 2014. **37**(11): p. 921-43.

56. James, A.W., et al., A Review of the Clinical Side Effects of Bone Morphogenetic Protein-2. Tissue Eng Part B Rev, 2016. **22**(4): p. 284-97.

57. Hemmer, B., et al., Minimal peptide length requirements for CD4+ T cell clones—implications for molecular mimicry and T cell survival Int Immunol, 2000. **12**(3): p. 375-83.

58. Aoki, K., et al., Peptide-based delivery to bone. Adv Drug Deliv Rev, 2012. **64**(12): p. 1220-38.

59. Molek, P., B. Strukelj, and T. Bratkovic, Peptide phage display as a tool for drug discovery: targeting membrane receptors. Molecules, 2011. **16**(1): p. 857-87.

60. Fosgerau, K. and T. Hoffmann, Peptide therapeutics: current status and future directions. Drug Discov Today, 2015. **20**(1): p. 122-8.

61. Sumigray, K.D. and T. Lechler, Cell adhesion in epidermal development and barrier formation. Curr Top Dev Biol, 2015. **112**: p. 383-414.

62. Reinhart-King, C.A., M. Dembo, and D.A. Hammer, The dynamics and mechanics of endothelial cell spreading. Biophys J, 2005. **89**(1): p. 676-89.

63. Bueter, C.L., C.A. Specht, and S.M. Levitz, Innate sensing of chitin and chitosan. PLoS Pathog, 2013. **9**(1): p. e1003080.

64. Jayakumar, R., et al., Biomaterials based on chitin and chitosan in wound dressing

applications. Biotechnol Adv, 2011. **29**(3): p. 322-37.

65. Crupi, A., et al., Inflammation in tissue engineering: The Janus between engraftment and rejection. Eur J Immunol, 2015. **45**(12): p. 3222-36.

66. Gonzalez, A.C., et al., Wound healing - A literature review. An Bras Dermatol, 2016. **91**(5): p. 614-20.

67. Arwert, E.N., E. Hoste, and F.M. Watt, Epithelial stem cells, wound healing and cancer. Nat Rev Cancer, 2012. **12**(3): p. 170-80.

68. Min, S.K., et al., The effect of a laminin-5-derived peptide coated onto chitin microfibers on re-epithelialization in early-stage wound healing. Biomaterials, 2010. **31**(17): p. 4725-30.

69. Gehlsen, K.R., et al., A synthetic peptide derived from the carboxy terminus of the laminin A chain represents a binding site for the alpha 3 beta 1 integrin. J Cell Biol, 1992. **117**(2): p. 449-59.

70. Wang, X., et al., The mouse excisional wound splinting model, including applications for stem cell transplantation. Nat Protoc, 2013. **8**(2): p. 302-9.

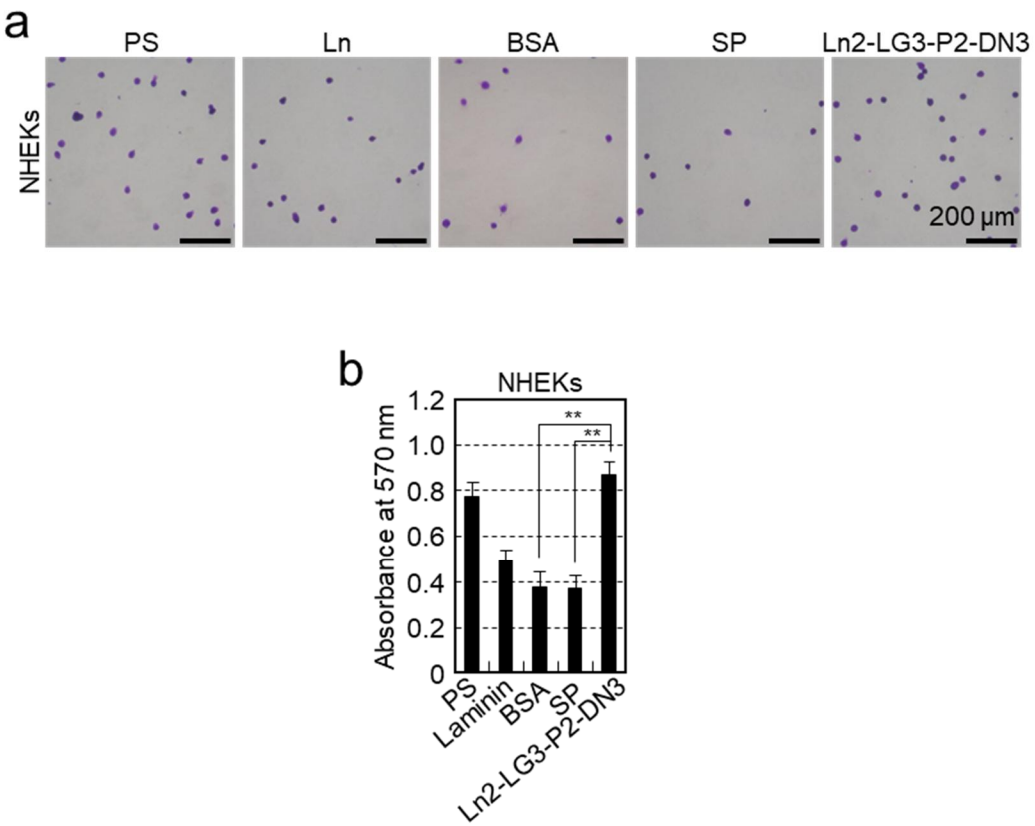

Figure 4. Cell attachment activities of normal human epidermal keratinocytes on coated dishes. a) Representative images of attached cells with different substrates. b) Attached cells are quantified by crystal violet staining. Ln2-LG3-P2-DN3-coated cell culture plate showed significantly increased cell attachment capacity compared to BSA- or SP-coated cell culture plate. Double asterisks indicate significant differences among them ($P < 0.01$, $n = 5$). NHEKs: Normal human epidermal keratinocytes, PS: Polystyrene, BSA: Bovine serum albumin, SP: Scrambled peptide.

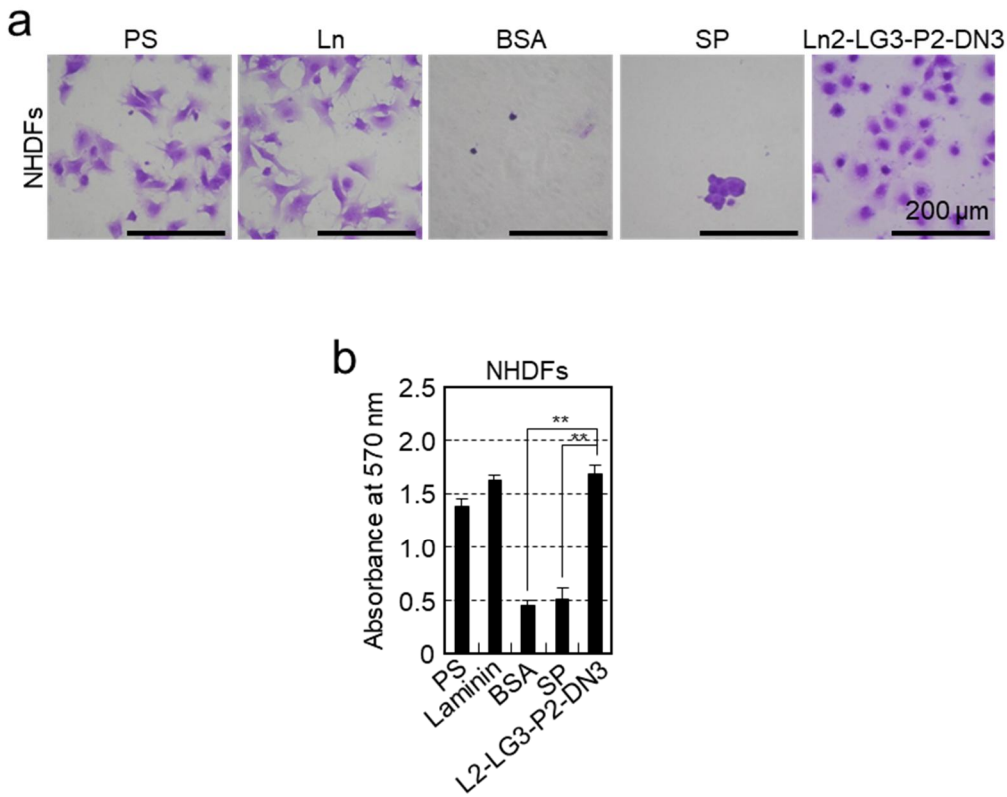

Figure 5. Cell attachment activities of normal human dermal fibroblasts on coated dishes. a) Representative images of attached cells with different substrates. b) Attached cells are quantified by crystal violet staining. Ln2-LG3-P2-DN3-coated cell culture plate showed significantly increased cell attachment capacity compared to BSA- or SP-coated cell culture plate. Double asterisks indicate significant differences among them ($P < 0.01$, $n = 5$). NHDFs: Normal human dermal fibroblasts, PS: Polystyrene, BSA: Bovine serum albumin, SP: Scrambled peptide.

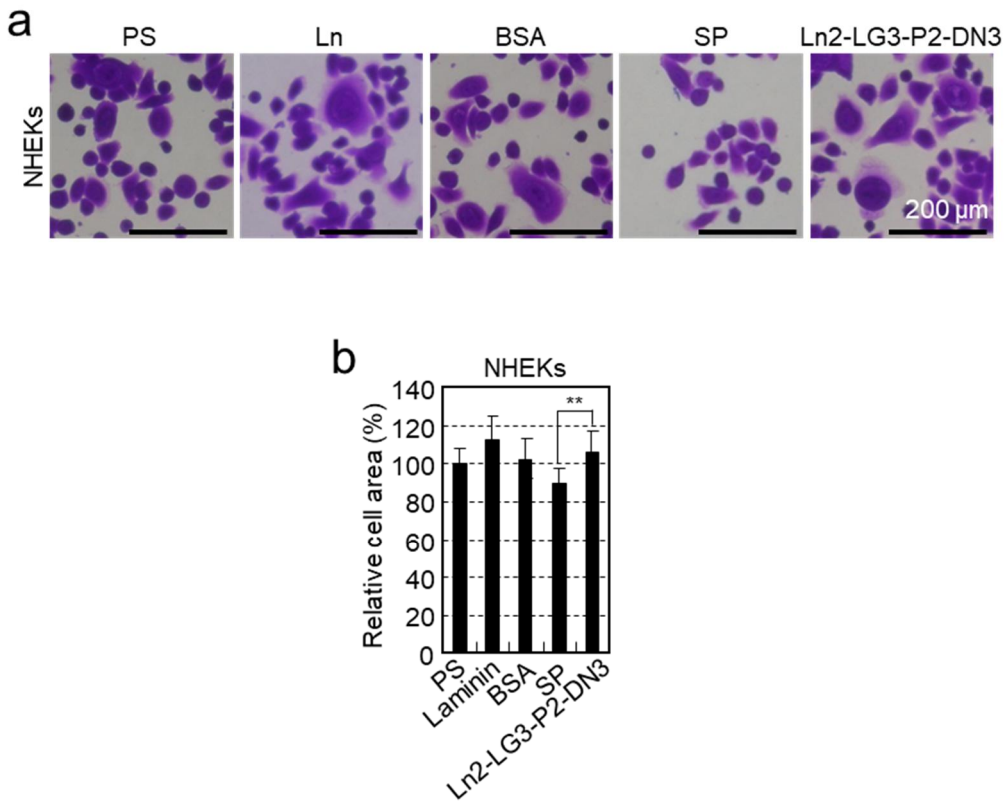

Figure 6. Cell spreading activities of normal human epidermal keratinocytes on coated dishes. a) Representative images of spread cells with different substrates. b) Spread cells are quantified by image measuring program. Ln2-LG3-P2-DN3-coated cell culture plate showed significantly increased cell spreading capacity compared to SP-coated cell culture plate. Double asterisk indicates a significant difference among them ($P < 0.01$, $n = 5$). NHEKs: Normal human epidermal keratinocytes, PS: Polystyrene, BSA: Bovine serum albumin, SP: Scrambled peptide.

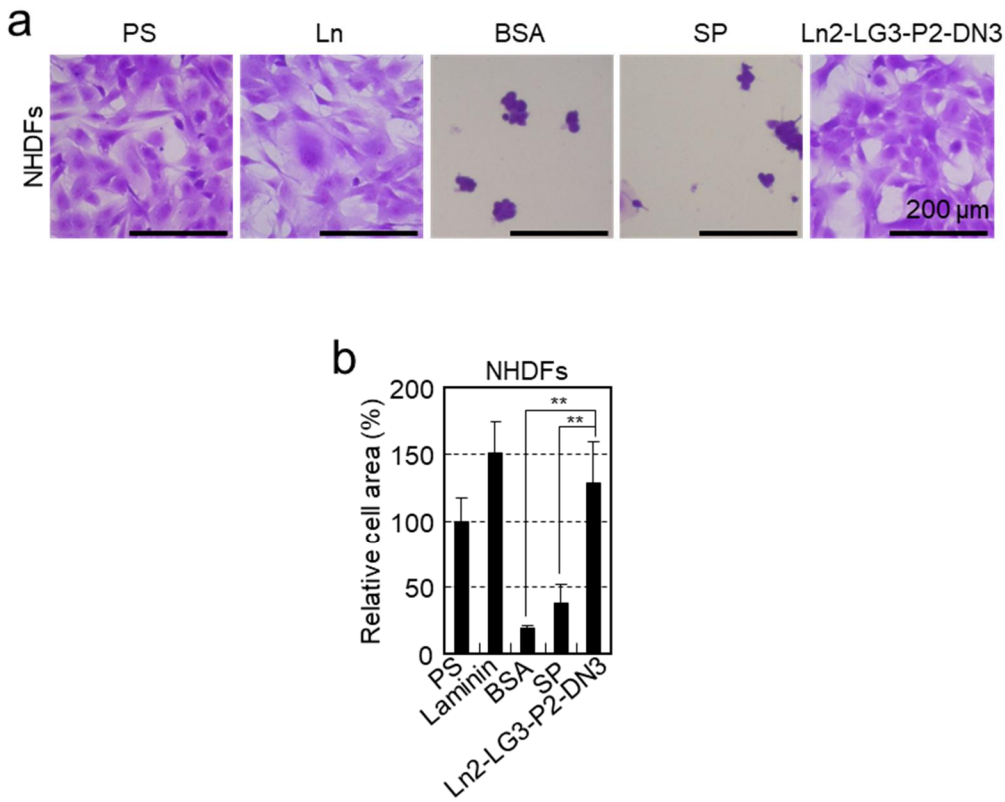

Figure 7. Cell spreading activities of normal human dermal fibroblasts on coated dishes. a) Representative images of spread cells with different substrates. b) Spread cells are quantified by image measuring program. Ln2-LG3-P2-DN3-coated cell culture plate showed significantly increased cell spreading capacity compared to BSA- or SP-coated cell culture plate. Double asterisks indicate significant differences among them ($P < 0.01$, $n = 5$). NHDFs: Normal human dermal fibroblasts, PS: Polystyrene, BSA: Bovine serum albumin, SP: Scrambled peptide.

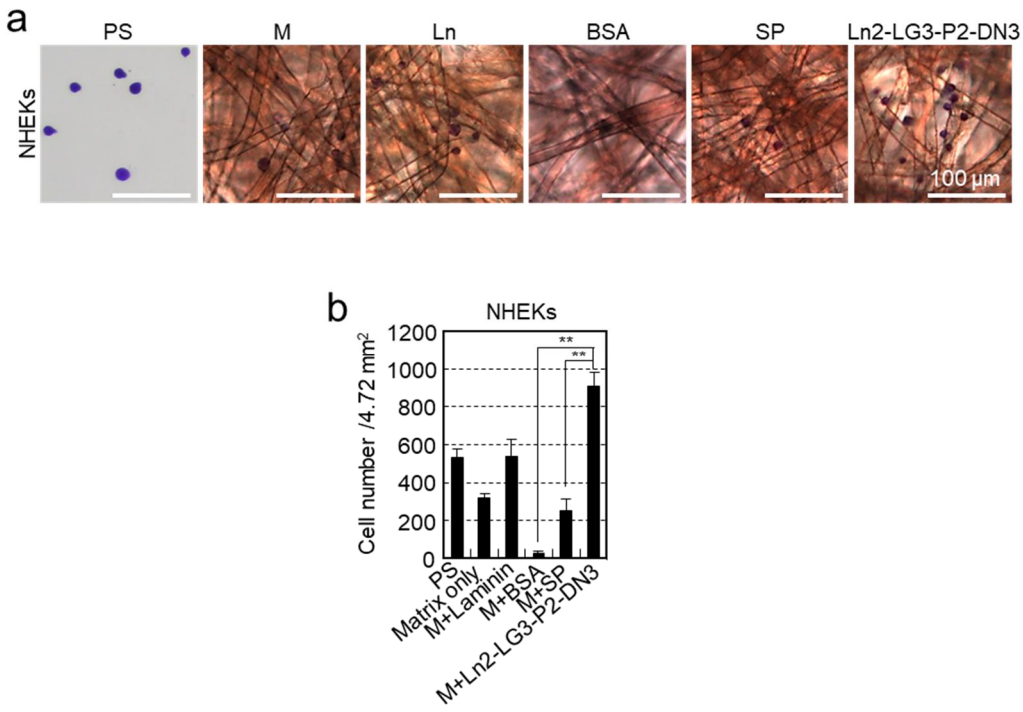

Figure 8. Cell attachment activities of normal human epidermal keratinocytes on coated chitin microfiber matrices. a) Representative images of attached cells with different substrates. b) Attached cells are quantified by counting stained cells. Ln2-LG3-P2-DN3-coated chitin matrix showed significantly increased cell attachment capacity compared to BSA- or SP-coated chitin matrices. Double asterisks indicate significant differences among them ($P < 0.01$, $n = 5$). NHEKs: Normal human epidermal keratinocytes, PS: Polystyrene, M, Matrix: Chitin microfiber matrix, BSA: Bovine serum albumin, SP: Scrambled peptide.

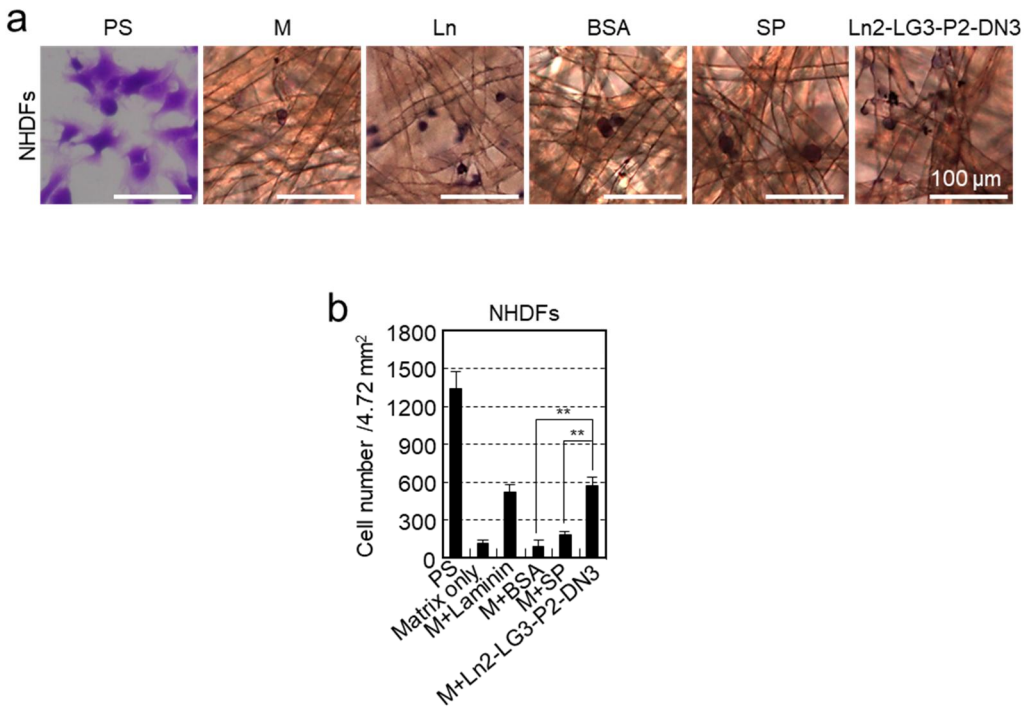

Figure 9. Cell attachment activities of normal human dermal fibroblasts on coated chitin microfiber matrices. a) Representative images of attached cells with different substrates. b) Attached cells are quantified by counting stained cells. Ln2-LG3-P2-DN3-coated chitin matrix showed significantly increased cell attachment capacity compared to BSA- or SP-coated chitin matrices. Double asterisks indicate significant differences among them ($P < 0.01$, $n = 5$). NHDFs: Normal human dermal fibroblasts, PS: Polystyrene, M, Matrix: Chitin microfiber matrix, BSA: Bovine serum albumin, SP: Scrambled peptide.

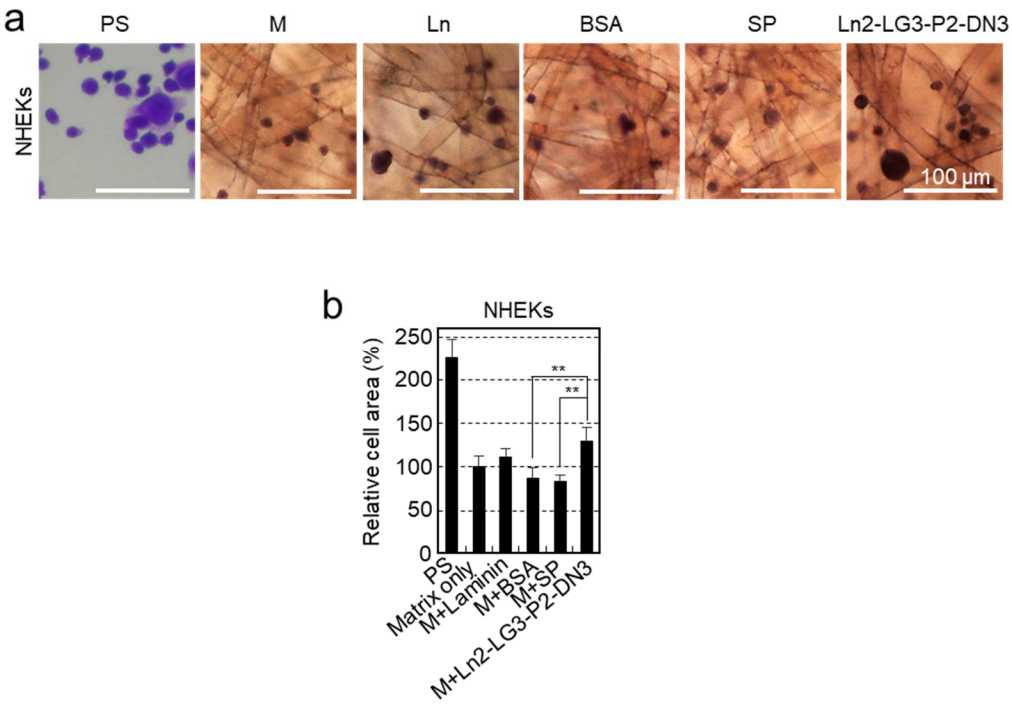

Figure 10. Cell spreading activities of normal human epidermal keratinocytes on coated chitin microfiber matrices. a) Representative images of spread cells with different substrates. b) Spread cells are quantified by image measuring program. Ln2-LG3-P2-DN3-coated chitin matrix showed significantly increased cell spreading capacity compared to BSA- or SP-coated chitin matrices. Double asterisks indicate significant differences among them ($P < 0.01$, $n = 5$). NHEKs: Normal human epidermal keratinocytes, PS: Polystyrene, M, Matrix: Chitin microfiber matrix, BSA: Bovine serum albumin, SP: Scrambled peptide.

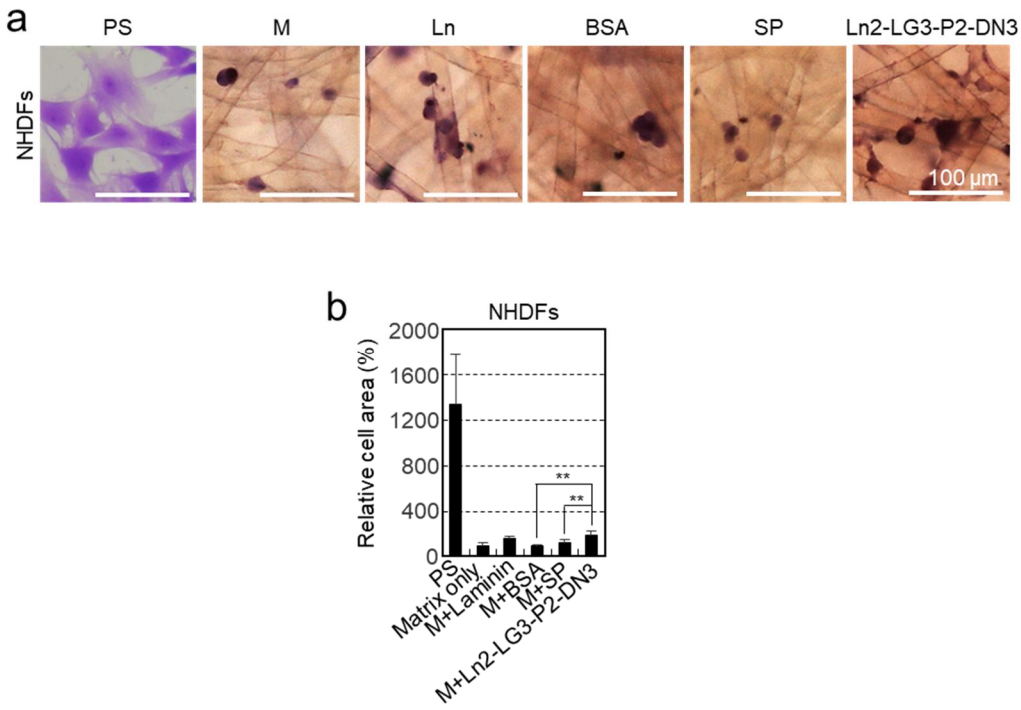

Figure 11. Cell spreading activities of normal human dermal fibroblasts on coated chitin microfiber matrices. a) Representative images of spread cells with different substrates. b) Spread cells are quantified by image measuring program. Ln2-LG3-P2-DN3-coated chitin matrix showed significantly increased cell spreading capacity compared to BSA- or SP-coated chitin matrices. Double asterisks indicate significant differences among them ($P < 0.01$, $n = 5$). NHDFs: Normal human dermal fibroblasts, PS: Polystyrene, M, Matrix: Chitin microfiber matrix, BSA: Bovine serum albumin, SP: Scrambled peptide.

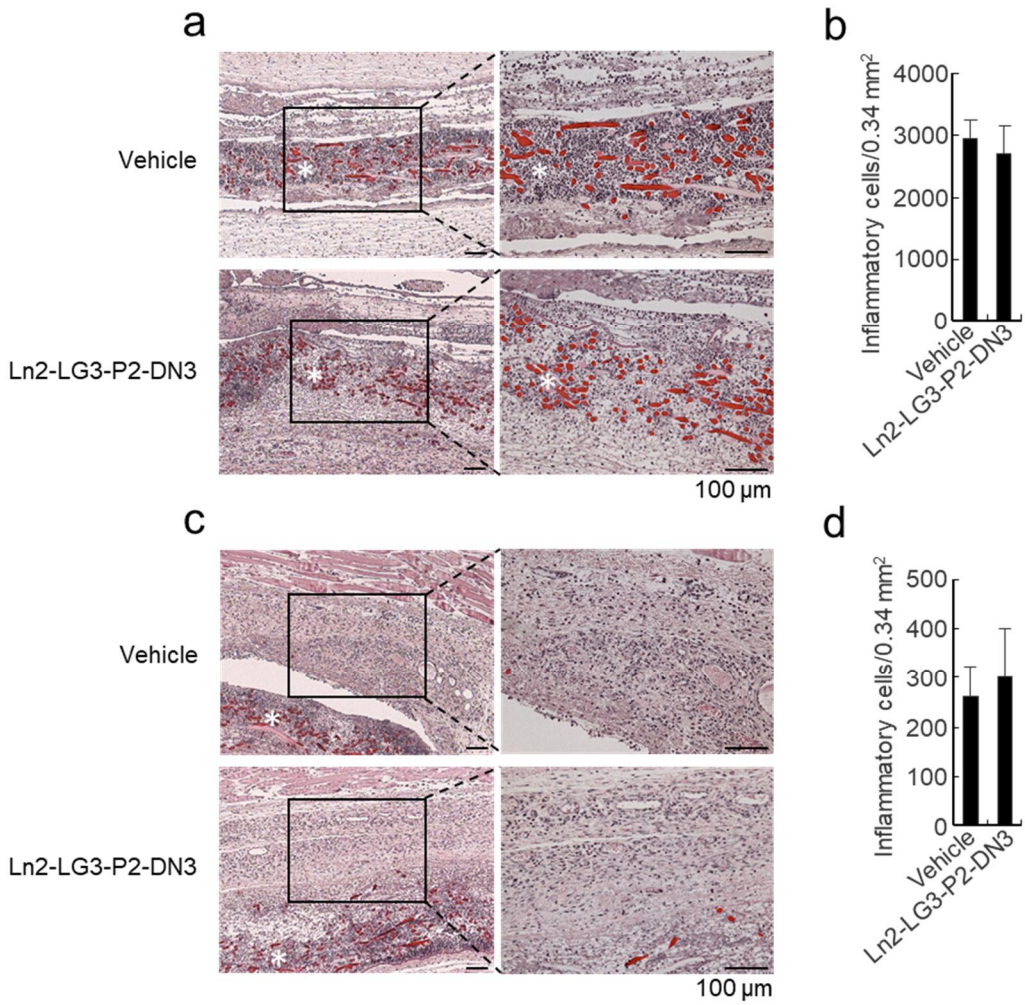

Figure 12. Representative photomicrographs and levels of inflammatory cells in cutaneous wounds of rats. Vehicle or Ln2-LG3-P2-DN3-treated Beschitin W matrices were implanted into subcutaneous regions of rat back skin for 3 days. H&E staining was performed in wounds inside (a) and around (c) the matrices, and inflammatory cells were counted in each wound (b, d). Scale bars, 100 μm. Insets are magnified images of the indicated rectangles. Data in (b) and (d) represent mean ± SD (n = 4 rats). *Chitin microfiber matrices.

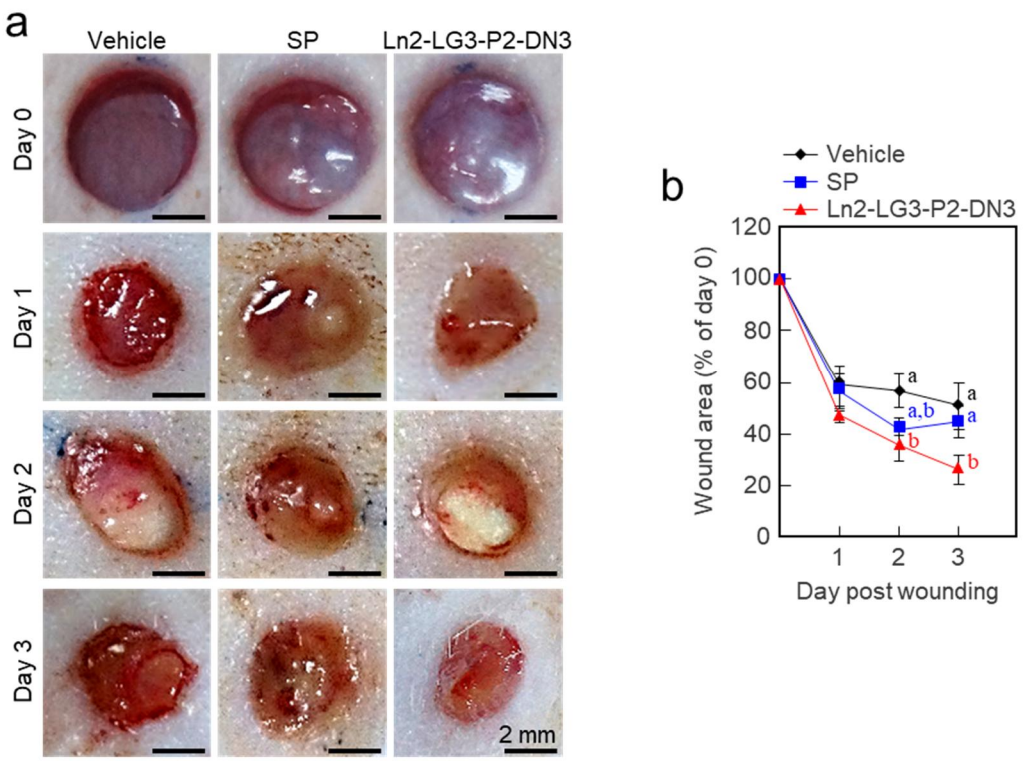

Figure 13. Acceleration of wound closure in the skins of Ln2-LG3-P2-DN3-treated wounds. a) Wound appearances treated with vehicle, SP-, or Ln2-LG3-P2-DN3-coated chitin microfiber matrices at day 1, 2, and 3 post wounding. b) Wound areas are quantified by image measuring program. The wounds tended to become smaller with Ln2-LG3-P2-DN3, compared to wounds with vehicle or SP. Different letters indicate significant differences among groups. There was no significant difference among groups in day 1. SP: Scrambled peptide.

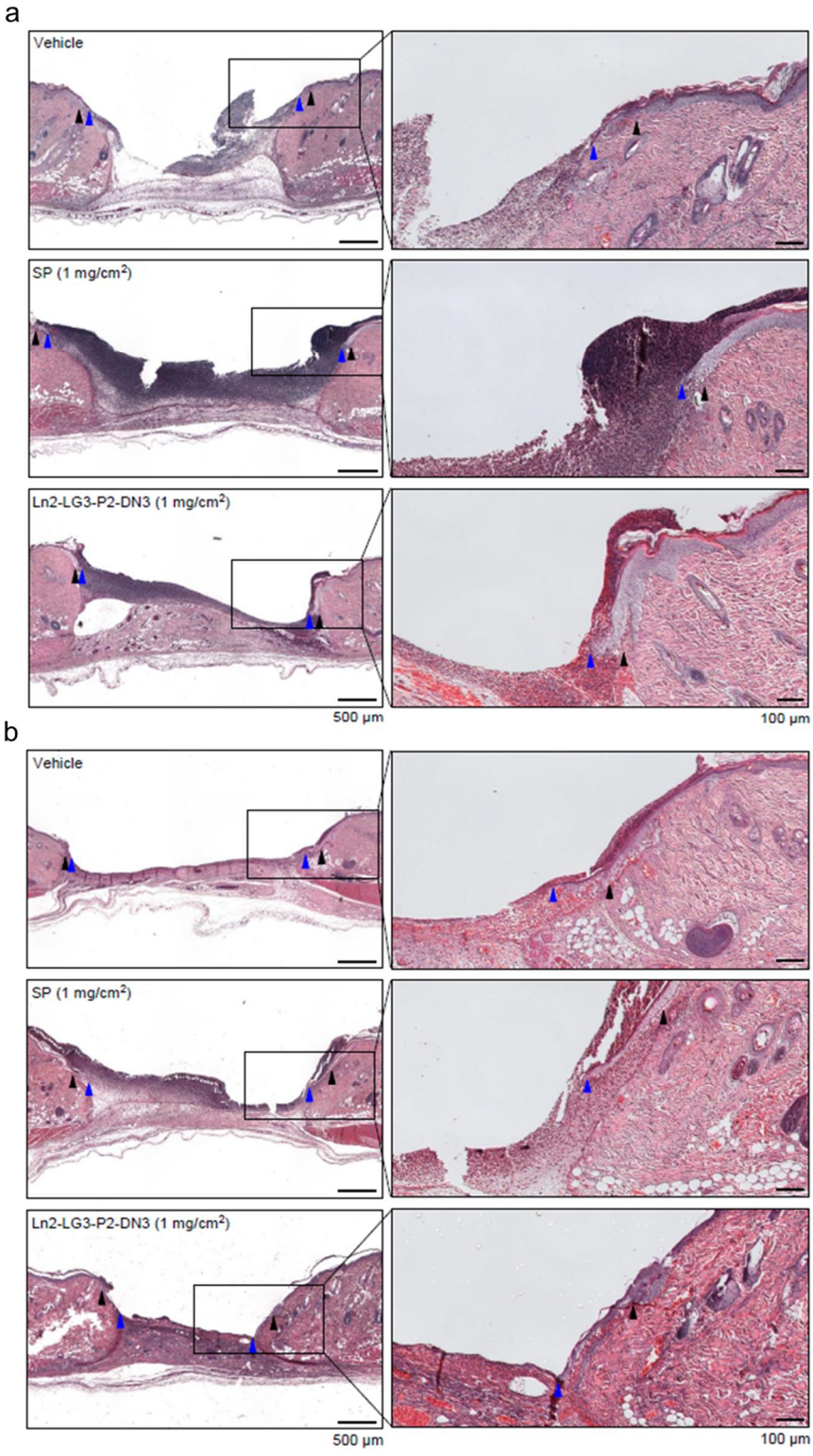
a
Vehicle
SP (1 mg/cm2)
Ln2-LG3-P2-DN3 (1 mg/cm2)
500 μm
100 μm
b
Vehicle
SP (1 mg/cm2)
Ln2-LG3-P2-DN3 (1 mg/cm2)
500 μm
100 μm

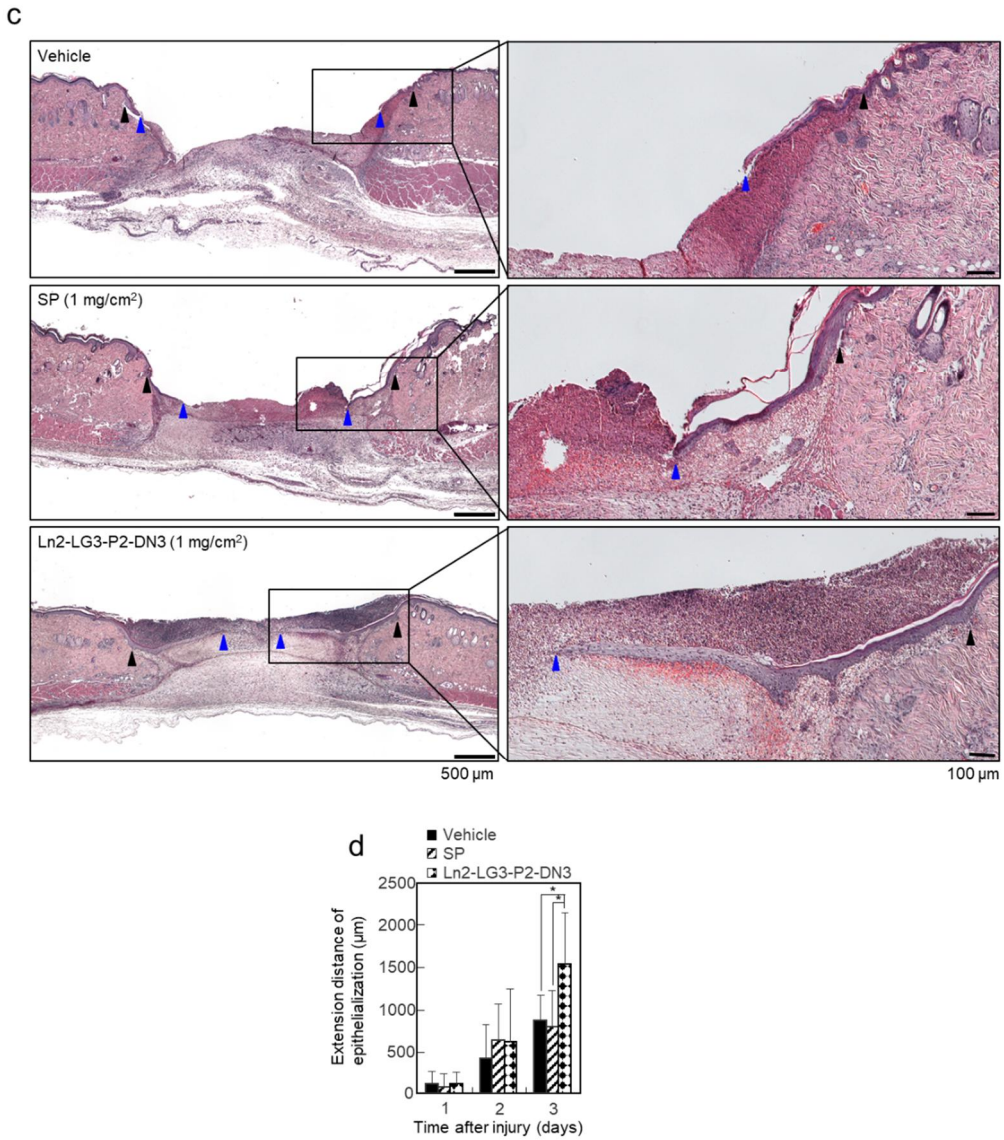

Figure 14. Acceleration of re-epithelization in the skins of Ln2-LG3-P2-DN3-treated wounds. a) Microscopic images of H&E stained rat skin samples treated with vehicle, SP-, or Ln2-LG3-P2-DN3-coated chitin microfiber matrices at day 1 post wounding. b) Microscopic images of H&E stained rat skin samples treated with vehicle, SP-, or Ln2-LG3-P2-DN3-coated chitin microfiber matrices at day 2 post wounding. c) Microscopic

images of H&E stained rat skin samples treated with vehicle, SP- or Ln2-LG3-P2-DN3-coated chitin microfiber matrices at day 3 post wounding. d) Re-epithelizations of vehicle, SP-, or Ln2-LG3-P2-DN3-treated wounds at day 1, 2 and 3 post wounding are quantified by image measuring program. Each length of re-epithelized tissues, from an original wound margin (black arrowhead) to an edge of epithelization (blue arrowhead) was verified and compared among groups. The Ln2-LG3-P2-DN3-treated wounds showed significantly increased re-epithelization compared to vehicle or SP-treated wounds. Asterisks indicate significant differences among them ($P < 0.05$, $n = 4$). SP: Scrambled peptide.

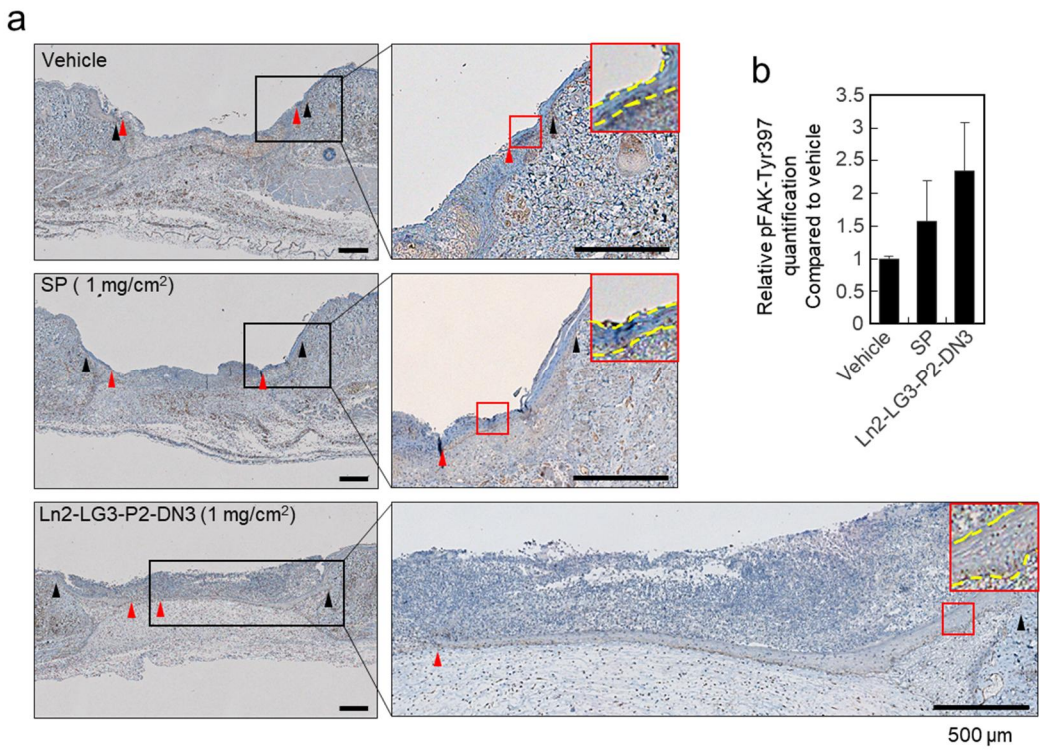

Figure 15. Phospho-FAK-Tyr397 expression of re-epithelized area in the skins of peptide-treated wounds. a) Microscopic images of phospho-FAK-Tyr397 stained rat skin samples treated with vehicle, SP-, or Ln2-LG3-P2-DN3-coated chitin microfiber matrices at day 3 post wounding. b) Phospho-FAK-Tyr397 of vehicle, SP-, or Ln2-LG3-P2-DN3-treated wounds at day 3 post wounding are quantified by image measuring program. Each area of re-epithelized tissues, from an original wound margin (black arrowhead) to an edge of epithelization (red arrowhead) was digitally cropped and staining intensity of each cropped image is verified with densitometric analysis using the plugin named as IHC profiler of Image-J software. The Ln2-LG3-P2-DN3-treated wounds showed increased tendency of phospho-FAK-Tyr397 compared to vehicle or SP-treated wounds. SP: Scrambled peptide.

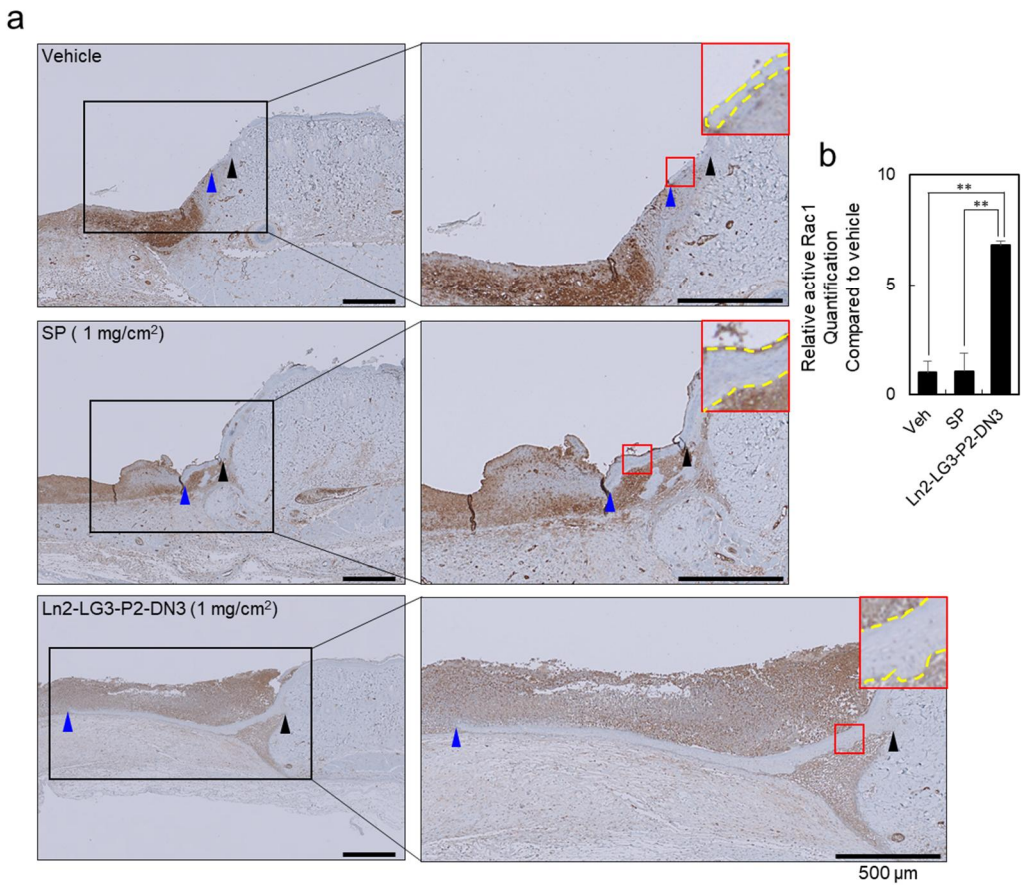

Figure 16. Active Rac1 expression of re-epithelized area in the skins of peptide-treated wounds. a) Microscopic images of active Rac1 stained rat skin samples treated with vehicle, SP-, or Ln2-LG3-P2-DN3-coated chitin microfiber matrices at day 3 post wounding. b) active Rac1 of vehicle, SP-, or Ln2-LG3-P2-DN3-treated wounds at day 3 post wounding are quantified by image measuring program. Each area of re-epithelized tissues, from an original wound margin (black arrowhead) to an edge of epithelization (red arrowhead) was digitally cropped and staining intensity of each cropped image is verified with densitometric analysis using the plugin named as IHC profiler of Image-J software. The Ln2-LG3-P2-DN3-treated wounds showed increased tendency of active Rac1

compared to vehicle or SP-treated wounds. Double asterisks indicate significant differences among them ($P < 0.01$, $n = 5$). SP: Scrambled peptide.

국문초록

라미닌-211 유래 펩티드가 피부창상 치유의 초기단계에서 재상피화에 미치는 영향

조 승 빈

종양 및 발달생물학 전공

서울대학교 대학원 치의과학과

(지도교수: 민 병 무, D.D.S., M.S., Ph.D.)

펩티드는 결손조직의 재생을 도모하고자 하는 조직재생 분야에서 유용한 과학적 수단으로서 주목받고 있다. 사람 라미닌 $\alpha 2$ 사슬에서 유래한 9개 아미노산잔기로 구성된 PPFEGCIWN 모티프 (잔기 2678-2686, Ln2-LG3-P2-DN3)는 피부 창상 치유에 주요한 사람 정상 피부각화세포와 사람 정상 피부섬유모세포의 세포부착을 촉진한다고 보고되었다. 그러나 *in vivo*에서 Ln2-LG3-P2-DN3 펩티드의 창상치유 효과는 아직 연구된 바 없었다. 그러므로 본 연구는 생체 내에서 Ln2-LG3-P2-DN3 펩티드가 재상피화 및 창상 폐쇄를 촉진시켜 피부창상 치유를 촉진할 수 있는지에 관하여 연구하였다. 세포적합성실험에서 Ln2-LG3-P2-DN3 펩티드는 배양접시 및 chitin microfiber matrix에 처리할 경우

vehicle이나 scrambled peptide를 처리한 경우보다 사람 정상 피부각화세포와 사람 정상 피부섬유모세포의 세포 부착과 퍼짐을 더욱 촉진시켰다. 흰쥐를 이용한 창상치유실험에서 피부창상 형성 후 2일과 3일째에 Ln2-LG3-P2-DN3 펩티드를 처리한 쥐의 창상 크기가 vehicle이나 scrambled peptide를 처리한 창상보다 현저히 감소하였다. 더욱이 Ln2-LG3-P2-DN3 펩티드를 처리한 쥐의 창상은 vehicle이나 scrambled peptide를 처리한 경우와 비교할 때 신속하게 재상피화가 일어났고, 이 과정에서 FAK-Tyr397 인산화와 Rac1의 활성화가 수반되었다. 또한 Ln2-LG3-P2-DN3 펩티드를 처리한 쥐와 vehicle을 처리한 쥐에서 염증세포 침윤을 비교하였을 때 염증세포 침윤에 유의한 차이를 보이지 않았다. 이러한 결과를 종합할 때, PPFEGCIWN 펩티드는 생체에서 창상 폐쇄와 재상피화를 촉진시켜 피부창상 치유를 촉진시키며, FAK-Tyr397과 Rac1의 활성화가 밀접히 관련되어 있음을 의미한다.

주요어: PPFEGCIWN 모티프, 세포거동, 재상피화, 창상 치유, phospho-FAK-Tyr397, Rac1-GTP, 백서 절제창상모델

학 번: 2015-22086